

Design of a Humanoid Biped for Walking Research

by

Daniel Joseph Paluska

Submitted to the Department of Mechanical Engineering
in partial fulfillment of the requirements for the degree of

Master of Science

at the

MASSACHUSETTS INSTITUTE OF TECHNOLOGY

September 2000

© Massachusetts Institute of Technology 2000

Signature of Author
Department of Mechanical Engineering
August 31, 2000

Certified by
Gill A. Pratt
Assistant Professor of Electrical Engineering and Computer Science, MIT
Thesis Supervisor

Certified by
Ernesto Blanco
Adjunct Professor of Mechanical Engineering, MIT
Thesis Supervisor

Accepted by
Ain Sonin
Chairman, Departmental Committee on Graduate Students

Design of a Humanoid Biped for Walking Research

by

Daniel Joseph Paluska

Submitted to the Department of Mechanical Engineering
on August 31, 2000, in partial fulfillment of the
requirements for the degree of
Master of Science

Abstract

This thesis presents the design of the robot M2. The primary motivation behind the work is to create a platform for research into bipedal walking. Bipedal robots have been built in the past, but most of them relied heavily on lessons from robotic arm research. There is evidence that suggests actuation and design for legged locomotion should deviate from the past standard of robotic arm design. Specifically, there should be an emphasis on low impedance actuation, shock tolerance, passive control mechanisms, and weight reduction. Human data which supports these points is presented.

The robot M2 was designed with these things in mind. M2 is a humanoid bipedal robot with twelve active degrees of freedom. It is essentially a torso and two legs and with linear dimensions of a 50th percentile US male. It weighs approximately 60 lbs(25kg). All the active degrees of freedom are powered using Series Elastic Actuators, which provide force control and shock tolerance. For simplicity, degrees of freedom above the hip are absent.

Thesis Supervisor: Gill A. Pratt

Title: Assistant Professor of Electrical Engineering and Computer Science, MIT

Thesis Supervisor: Ernesto Blanco

Title: Adjunct Professor of Mechanical Engineering, MIT

Acknowledgments

The development of the robot has been a three person project from the beginning. Jerry Pratt and David Robinson worked on the robot with me. Jerry performed preliminary simulations to determine feasibility of mass distributions and power requirements. David Robinson is responsible for the actuator design. I also had lots of help from Ben Krupp and Chris Morse who each had there own robot to build in the process. Pete Dilworth contributed plenty of tips from his own bipedal robot building experience. Allen Parseghian has been working hard with me trying to get the robot to actually walk. John Hurst has helped with debugging some actuator problems and designing a battery rig. Thanks to Mike Wessler and Andreas Hofmann for creation of and help with software tools. Thanks to Chris Barnhart for developing the DSP platform and handling my ignorance of all things DSP.

During the construction, I had help from many people. We had several soldering parties in the lab which involved people sitting around the main lab table soldering. Jerry, Ben, Chris, Mike, Gaddy, Pete, and others participated in these. In addition, Jess helped me with cable making and was an immense help with my supposed native language.

Professor Pratt has been a wonderful advisor. I am constantly amazed at how he has always placed his students first. I have loved working in the lab and getting to play around!

Special thanks goes to my friends and family who have made the time outside the lab great! You've kept me sane during the worst of thesis despair.

Contents

1	Introduction	9
1.1	Goals of Thesis	9
1.2	Summary of Thesis	10
2	Human Characteristics	11
2.1	The Human Form	11
2.1.1	Weight Distribution	11
2.1.2	Link Lengths	11
2.2	Human Motion	14
2.2.1	Energetics of Human Walking	14
2.2.2	Human Kinetic and Kinematic Data	15
3	Robots and Actuators	16
3.1	Robotic Arms vs. Robotic Walkers	16
3.2	Passive Dynamic Walkers	16
3.3	Powered Bipedal Walkers	17
3.4	Series Elastic Actuators	17
4	Robot Mechanical Design	19
4.1	General Robot Architecture	19
4.2	The Design	19
4.2.1	Overall Structure	19
4.2.2	Actuators	22
4.2.3	Ankle	22
4.2.4	Foot	22
4.2.5	Hip	24
4.2.6	Knee	25
5	Electronics and Control Systems	27
5.1	Electronics Overview	27
5.1.1	48 Volt bus	27
5.1.2	Robot Sensors	27
5.2	Custom Circuit Boards	29
5.2.1	The Signal Conditioning Boards	29
5.2.2	The Analog Force Control Boards	29
5.2.3	The Analog Breakout Board	31
5.2.4	The Power Distribution Boards	31
5.2.5	The DSP and Analog I/O	31
5.3	Control Software	31

A Joint Math	34
A.1 Knee Joint	34
A.2 Ankle Joint	36
A.3 Hip Joint	37
A.3.1 Hip Pitch	37
A.3.2 Hip Roll and Yaw	37
B Electrical Schematics	39
C Suppliers and Costs	50
C.1 Costs	53

List of Figures

2-1	The X velocities of the various parts of the body during a normal walking cycle. Adapted from data in Winter(20).	12
2-2	The frontal plane dimensions of a 50th percentile U.S. male. Adapted from data in Dreyfus(2). All dimensions are in inches.	13
2-3	Several strides of the compass gait shown with corresponding potential and kinetic energy curves. From Krupp(8).	14
3-1	Some previous powered bipedal walking robots.	17
3-2	An annotated rendering of the Series Elastic Actuator which is used in the robot M2. Modeled and rendered by David Robinson.	18
4-1	A photo of the completed robot and a joint schematic view of the robot. The schematic shows active degrees of freedom only. The optional passive toe joint is not shown.	20
4-2	The dimensions of the biped in the frontal plane. The body and links are approximately axially symmetric about their longitudinal axis. Dimensions are in inches.	21
4-3	A schematic of the ankle joint actuation scheme. The axes shown are fixed to the center of the universal joint. The points A,E, and O are referenced in Appendix A.	23
4-4	The dimensions of the biped foot with passive toe joint. The X's represent the location of the load cells.	23
4-5	A schematic of the biped hip. The pitch actuator is not shown. It lies along the axis of the thigh.	24
4-6	A photo of the biped thigh illustrating the hip pitch cable drive system.	24
4-7	The ranges of motion on the robot ankle joint. The ankle roll is symmetric(± 20 deg).	25
4-8	The range of motion of the robot knee. The knee has 80 degrees of motion.	26
5-1	An overview of the biped electronics. Thick lines indicate power transfer and arrowheads indicate information flow.	28
5-2	A photo of M2 with annotations of electrical systems.	29
5-3	A photo of the biped strain gauge signal conditioning board. This board handles two strain gauges. There are a total of four of these boards on the robot.	30
5-4	A photo of the analog force control and joint pot buffer board. There are six identical boards on the robot.	30
A-1	The robot knee joint with superimposed lines and points. Points O, A and M all refer to pin joints. O is the knee joint. M is where the actuator is mounted to the thigh and A is where the actuator is attached to the shin.	35
A-2	A line drawing of the knee for the calculation of knee actuator desired force. The actuator is the line segment \vec{MA} . This drawing also pertains to the geometry of the hip and ankle joints but the hip and ankle actuators have motions out of the plane whereas the knee actuator is always in the plane perpendicular to the knee axis.	35

A-3 A simple view of the actuation of the robot ankle. This is a tranverse plane slice of the robot ankle. Point O is the intersection of the X and Y axes as well as the center of the ankle universal joint. Points A1 and A2 represent the attachment points of the two actuators respectively. Forces in the actuators create torques about both the X and Y axes. Joint rotations change the relative lengths of the X and Y projections(r_x and r_y) of the moment arms, therefore affecting the torque to force transformation. 36

A-4 The robot hip joint schematic. Point O refers to the hip universal joint. The Z(hip yaw) and Y(hip roll) axes intersect at point O. Point M_r refers to the universal joint on the body where the roll actuator is mounted. Point A_r refers to the ball joint on the thigh where the roll actuator is attached. Point M_y refers to the pin joint where the yaw actuator is attached to body. Point A_y is the pin joint attachment of the yaw actuator to the yaw universal block. It is hidden in this schematic. 37

B-1 Page 1 of 6 of the biped force board. 40

B-2 Page 2 of 6 the biped force board. 41

B-3 Page 3 of 6 of the biped force board. 42

B-4 Page 4 of 6 the biped force board. 43

B-5 Page 5 of 6 of the biped force board. 44

B-6 Page 6 of 6 the biped force board. 45

B-7 Page 1 of 2 of the strain gauge conditioning board. 46

B-8 Page 2 of 2 of the strain gauge conditioning board. 47

B-9 Page 1 of 1 of the analog I/O breakout board. This board is designed to interface with the ANA070 and ANA064 from Digital Designs and Systems. 48

B-10 Page 1 of 1 of the M2 power distribution board. This board has two different population options. One to power the DSP and one to power the Intersense IS-300 tracker. 49

List of Tables

2.1	Human Mass Distribution. From Dempster(3).	11
2.2	Human walking parameters from normalized data contained in <u>Human Walking</u> (18). Forces and power calculated for a for 1.83 m(6'2"), 80 kg(178lb) person. Table displays non-concurrent maximum values which occur during an average walking cycle. . . .	15
4.1	Robot Joint Specifications. Torque and rad/s numbers are given for maximum moment arm. Power, torque, and velocity are symmetric due to the actuator. *The ankle roll and pitch are not independent. Their maximum values can not be applied simultaneously.	19
4.2	Approximate distribution of mass in humans, the biped M2, and McGeer's kneed passive dynamic walker(PDW). Human data adapted from Dempster and Gaughran (3). Robot weight distribution is driven primarily by actuator locations. Each actuator is approximately 1.2kg(2.5 lbs).	22
5.1	Circuit Boards on the Robot	27
5.2	Sensors on the Robot	28
C.1	Basic robot budget. See Robinson et al.((17)) for more detail on the actuator. This budget does not include prototyping or development costs. Part quantities and individual costs are not necessarily meant to imply identical parts but rather to give an average price for all units of a certain type.	54

Chapter 1

Introduction

1.1 Goals of Thesis

The goal of this research project was to design a three dimensional, free standing bipedal robot. The main goal of the biped, M2, is to be a testbed for control ideas and walking research. Originally the robot was not specifically 'humanoid,' but after a bit of research we determined it would be the best course of action for several reasons.

- There is a vast amount of data regarding human form and motion.
- The robot can be considered a human replacement for hazardous situations.
- The robot will be large enough to avoid problems of miniaturization.
- Ideas regarding human control of locomotion can be tested.

This thesis concentrates on documenting the mechanical portion of the project. The design of the robot was guided by several specific goals which include walking 1 m/s, climbing normal stairs, looking biological, turning dynamically, a three year life-span, and ten hours working time between mechanical or electrical failures.

The following points dominated the design decisions of the robot.

1. **Series Elastic Actuators** Series Elastic Actuators(12) are used for all of the active degrees of freedom. These actuators provide force control as well as shock tolerance. Evidence suggests both factors are necessary for the task of biologically similar walking. The low output impedance of the actuators allows us to take advantage of the robot's natural dynamics. All joints employ the same actuator design to minimize complexity and facilitate repairs.
2. **Human Proportions** The use of human proportions allows for easy comparison with biomechanics data. Human sizing also allows for use of large, standard components which are easy to see and debug. Also, by using human proportions, the research stays focused on walking and not on miniaturization.
3. **Lightweight** The robot frame is carbon fiber and most other components are plastic or aluminum. The necessary actuator forces are kept low. A less massive robot is more manageable in a research environment. It is easier to handle and less likely to damage itself or harm researchers.
4. **Mechanical Control Mechanisms** Each joint (most importantly the knee) has adjustable stops with rubber pads. The foot of the robot is equipped with a passive toe joint. This joint has an adjustable range as well as a return spring. The limit stops are essentially high frequency non-linear PD loops which are difficult to implement in digital control even with the use of sophisticated electronics and sensors. The low impedance actuators allow for uncertain

contact, an inevitable occurrence during walking on rough terrain. These mechanical features eliminate the need to operate any digital high frequency control loops on the robot.

The robot is a three dimensional continuation of the work that began with the planar robot Spring Turkey(13) and continued with the planar robot Spring Flamingo(15). The previously enumerated points are the key areas where M2 differs from some other current three dimensional humanoid walkers(6, 21) which rely more on high impedance actuation and trajectory following control schemes.

1.2 Summary of Thesis

This thesis presents the design of the humanoid robot M2.

- Chapter 2 describes the human mechanisms and the forces, torques, velocities, etc. which are exhibited during a normal walking cycle. The human is a good starting point for the design of the robot. Human locomotion is well documented and there is a wealth of information on the human walking motion.
- Chapter 3 describes previous robots and actuators. It presents some of the differences between robotic arm and walking robot technology. There is a brief introduction to Series Elastic Actuators.
- Chapter 4 describes the mechanical specifics of the robot.
- Chapter 5 details the electronic, sensor, computer, and control systems on the robot.
- Chapter 6 gives some conclusions and some advice for future research.
- Appendix A describes the transformations from joint torques to actuator linear forces.
- Appendix B contains all the schematics for the custom circuit boards on the robot.
- Appendix C has a list of all of the suppliers that were used.

Chapter 2

Human Characteristics

There is a large database of knowledge regarding both the human form and human motion. We believe that mechanical characteristics found in humans aid in the control of walking and we should try to consider which of these characteristics can be embodied with current mechanical and robotic technologies.

2.1 The Human Form

2.1.1 Weight Distribution

An approximation of the human weight distribution is shown in Table 2.1.

From this we can see that nearly 70% of the mass in humans is located at the waist and above. Figure 2-1 shows the linear velocities (in the walking direction, X) of different body areas. It can be seen that the body has the least fluctuation in forward velocity and the foot has the most fluctuation.

Since kinetic energy is a direct function of velocity, the lower extremities have the greatest fluctuations in kinetic energy. It is clear that more mass at the feet means more energy change. If this energy is all lost it would be very costly. In efficient walking, the mass is able to resonate with gravitational or elastic potential energy. An example of this can be seen in the compass gait described in the next section.

2.1.2 Link Lengths

The dimensions of a 50th percentile male are shown in Figure 2-2. The center of gravity is just above the hip at approximately 38".

Table 2.1: Human Mass Distribution. From Dempster(3).

Body Area	Percentage per Part	No. of Instances	Total Mass Percentage
Head, neck, Shoulders, Thorax	31%	1	31%
Arm	5%	2	10%
Ab/Pelvic	27%	1	27%
Thigh	10%	2	20%
Shin and foot	6%	2	12%

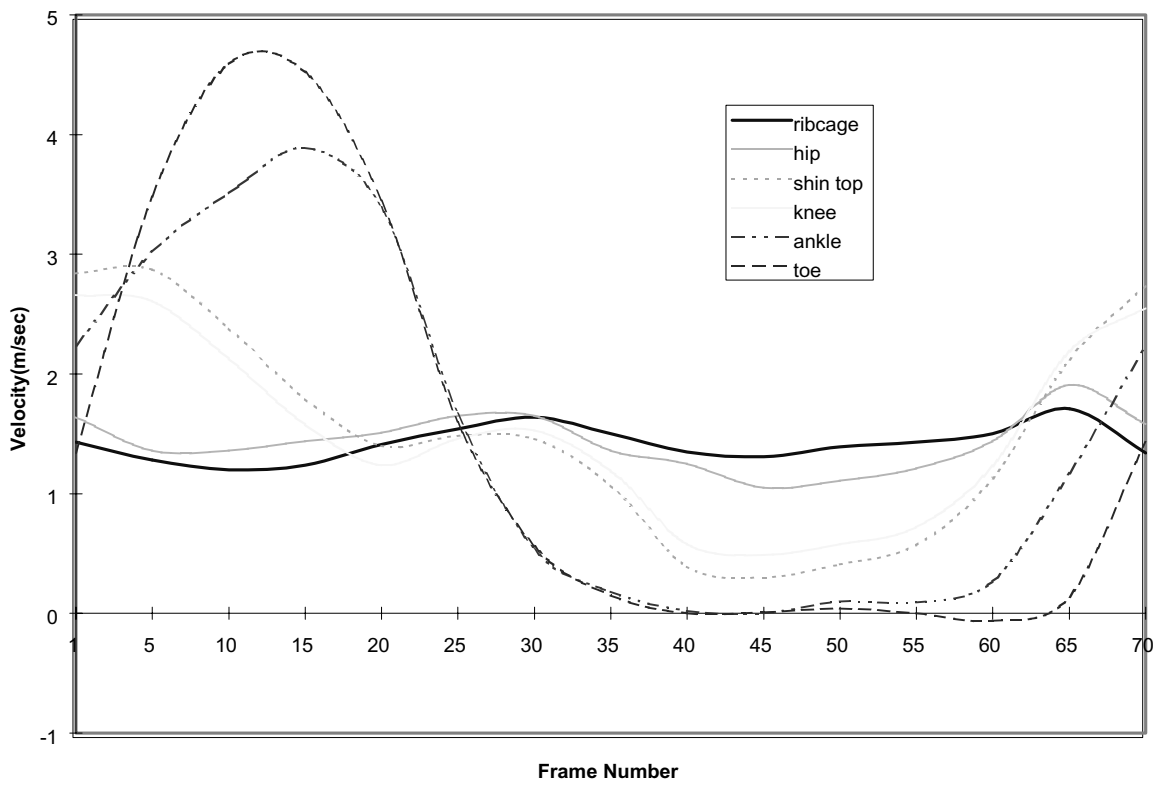


Figure 2-1: The X velocities of the various parts of the body during a normal walking cycle. Adapted from data in Winter(20).

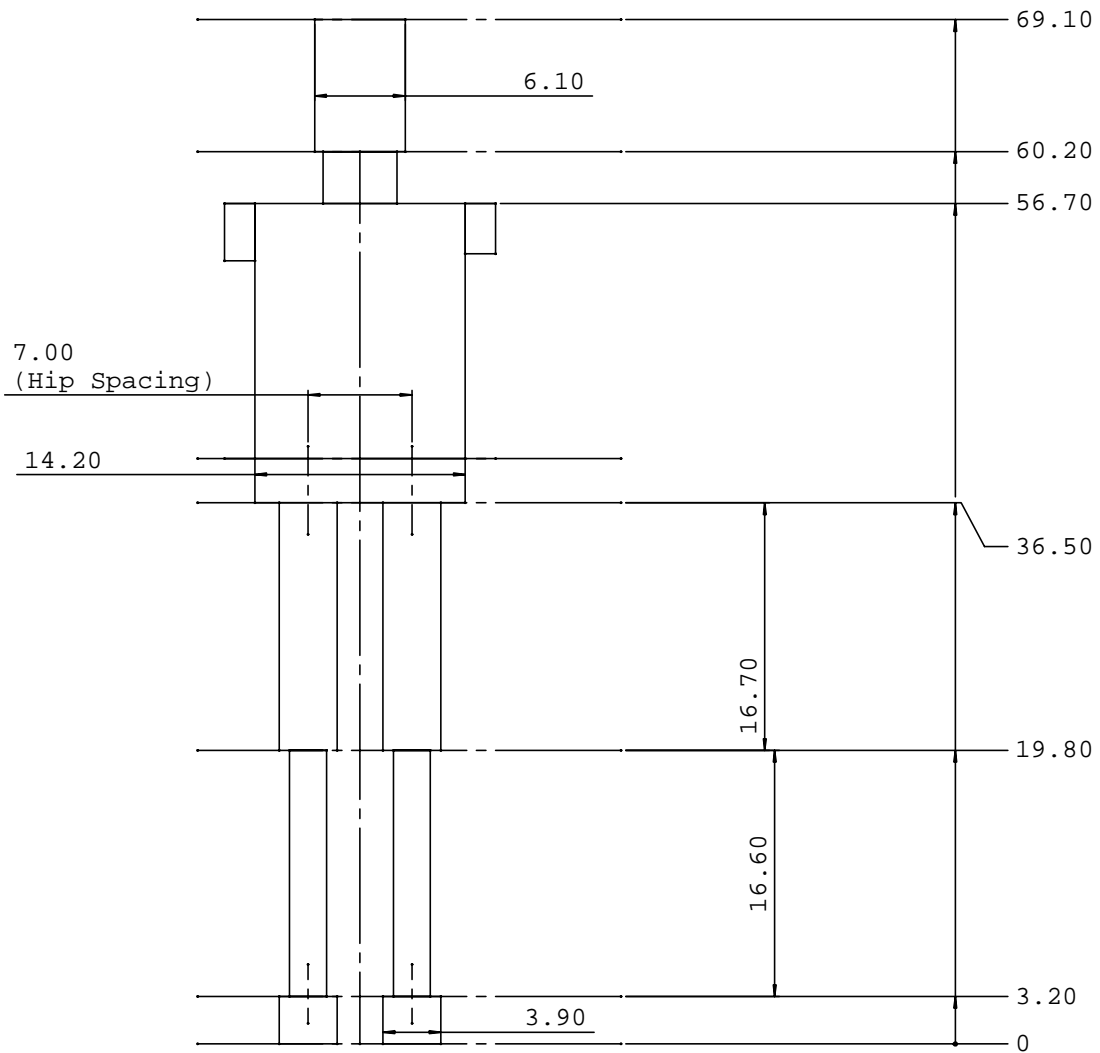


Figure 2-2: The frontal plane dimensions of a 50th percentile U.S. male. Adapted from data in Dreyfus(2). All dimensions are in inches.

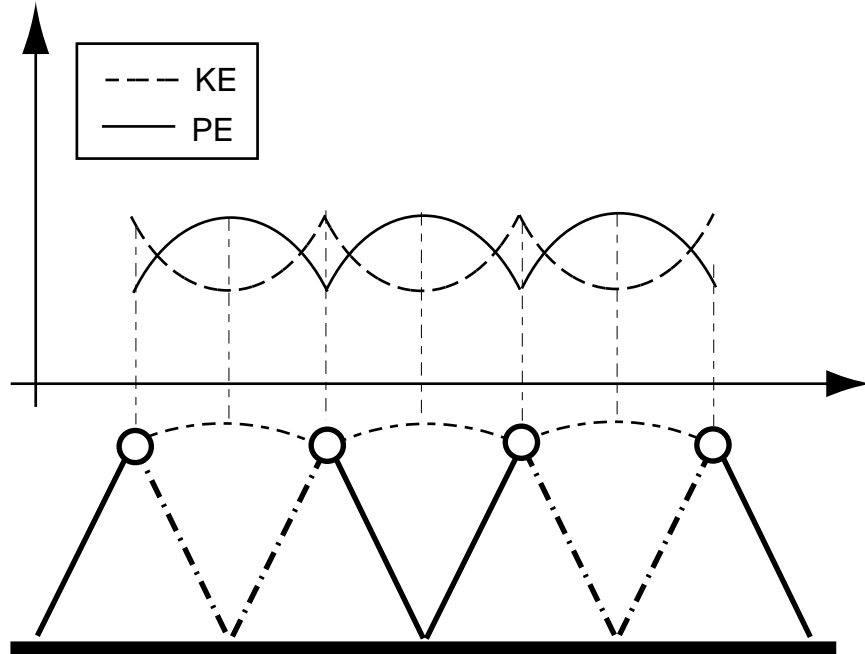


Figure 2-3: Several strides of the compass gait shown with corresponding potential and kinetic energy curves. From Krupp(8).

2.2 Human Motion

2.2.1 Energetics of Human Walking

Data in Rose et al.(18) shows us that a 180lb person walking at a normal pace consumes about 320 Watts of power. It is estimated that roughly one quarter of that is mechanical power. This means that at a comfortable pace, a 180lb human can walk with only 80 Watts of mechanical power. This can be a somewhat depressing fact considering one of the electric motors used on the robot M2 can output 90 Watts continuously - and there are 12 motors on the robot! Hopefully research on M2 will allow future robots to walk as mechanically efficient as a human.

A simplified human gait known as a compass gait can give us insight into the energetics of walking. The compass gait model consists of two rigid, massless legs attached at the hip with a pin joint. A point mass is modeled at the hip joint. With the only degree of freedom located at the hip, the body is forced to follow an arc defined by the length of the leg. The compass gait can be seen in Figure 2-3.

The compass biped has instantaneous, discretely changing dynamics. It simply changes from one inverted pendulum to another when the swing leg touches the ground. Calculating the external work on the model, namely the potential and kinetic energy of the system

$$PE = MgL\cos\theta \tag{2.1}$$

$$KE = MgL(1 - \cos\theta) \tag{2.2}$$

By graphing the equations 2.1 and 2.2 in Figure 2-3, the cyclical nature of potential energy and kinetic energy can be seen. Note that the kinetic energy is maximum when the potential energy is minimum and vice versa. Similar cyclical transition of potential and kinetic energy was recorded

	deg	rad/s	Nm	W
hip(pitch)	30,-18	3.6,-2.0	-111.0	56
hip(roll)	8,-7	1.6,-1.0	-63.5	+28
hip(yaw)	5,-15	4.0,-3.0	8.0	-16
knee(pitch)	68,8	5.8,-7.8	-71.4	-79.5
ankle(pitch)	10,-15	3.0,-4.2	-63.5	280
ankle(roll)	na	NA	40.0	-16

Table 2.2: Human walking parameters from normalized data contained in Human Walking(18). Forces and power calculated for a for 1.83 m(6'2"), 80 kg(178lb) person. Table displays non-concurrent maximum values which occur during an average walking cycle.

in human subjects by McMahan (11) using force plate data to calculate the changes in mechanical energy of the body's center of mass.

The compass gait is similar to the behavior found in the passive dynamic walkers described in the next section. There is also evidence that humans use some passive dynamics during the gait cycle. At the beginning of swing phase, the leg receives a tiny impulse of energy and then the natural pendulum motion carries it forward to extension. The leg receives another tiny impulse of energy to bring it to a sudden halt before touchdown. Electromyographic data record by McMahan (11) shows little electrical activity in the leg muscles of humans during the swing phase at normal walking speeds. This suggests that the leg is swinging freely during this period. In addition, electromyographic records show significant electrical activity in leg muscles during stance.

2.2.2 Human Kinetic and Kinematic Data

There is a wealth of data from recordings of human motion. These recordings have been transferred into data regarding joint motions and joint torques during the walking cycle. In addition, the author relied on a rather low-tech method for extracting velocity data from the graphical position data. Power, torque, position, and velocity data for an average human walking cycle are shown in Table 2.2.

Chapter 3

Robots and Actuators

3.1 Robotic Arms vs. Robotic Walkers

Many high performance robotic arms and hands have been developed for use in factories, space, and research(19). It might seem to an outside observer that these technologies could be exploited for use in a legged robot. Most of the time this is not the case. There are several reasons why.

- **Fixed vs. Floating Reference** Robotic arms are generally fixed to an inertial reference frame(factory) or a body whose mass is large enough that it can be considered fixed(spacecraft). A walking robot is not fixed to any reference frame and has a limited set of torques which it can apply due to its limited contact with the world.
- **Onboard vs. Offboard** Robot arms can often place their heavy motors at their fixed end. Then the motors are only responsible for moving the frame of the arm and not themselves. Because a walking robot must carry all its components, the motors support themselves as well as the structure of the robot. Carrying power is also an issue for walking robots although most are tethered due to battery limitations.
- **Environmental Awareness** Robot arms are not usually expected to perform in unknown situations. They generally are designed for specific working conditions and their ability to handle unexpected disturbances is limited. Ideally, walking robots are supposed to handle rough and unknown terrain.
- **Success Metrics** Robotic arms are often judged on their ability to position their end effectors precisely. Robotic walkers are usually not judged on their ability to position precisely but rather on their ability to get from Point A to Point B without falling down.
- **Impacts** Most robot arms are not designed to handle impacts. Walking, however, has an impact at every touchdown.

3.2 Passive Dynamic Walkers

Much research has been done on completely passive walking machines (5, 1, 4). Passive dynamic walkers use Earth's gravity as a power supply. They rely on special geometry and mechanical mechanisms as control systems to achieve gaits very similar to the compass gait depicted in Figure 2-3. Though they are not robots in the traditional sense, they can give insight into walking machines. These 'robots' exploit passive dynamic elements and mechanical mechanisms to achieve highly efficient gaits. In the limit, a passive dynamic walker relies entirely on passive dynamic motions and thus requires no external power source other than a small incline. Several passive legged 'robots' such as these have been constructed and successfully demonstrated (5, 1, 4, 9).

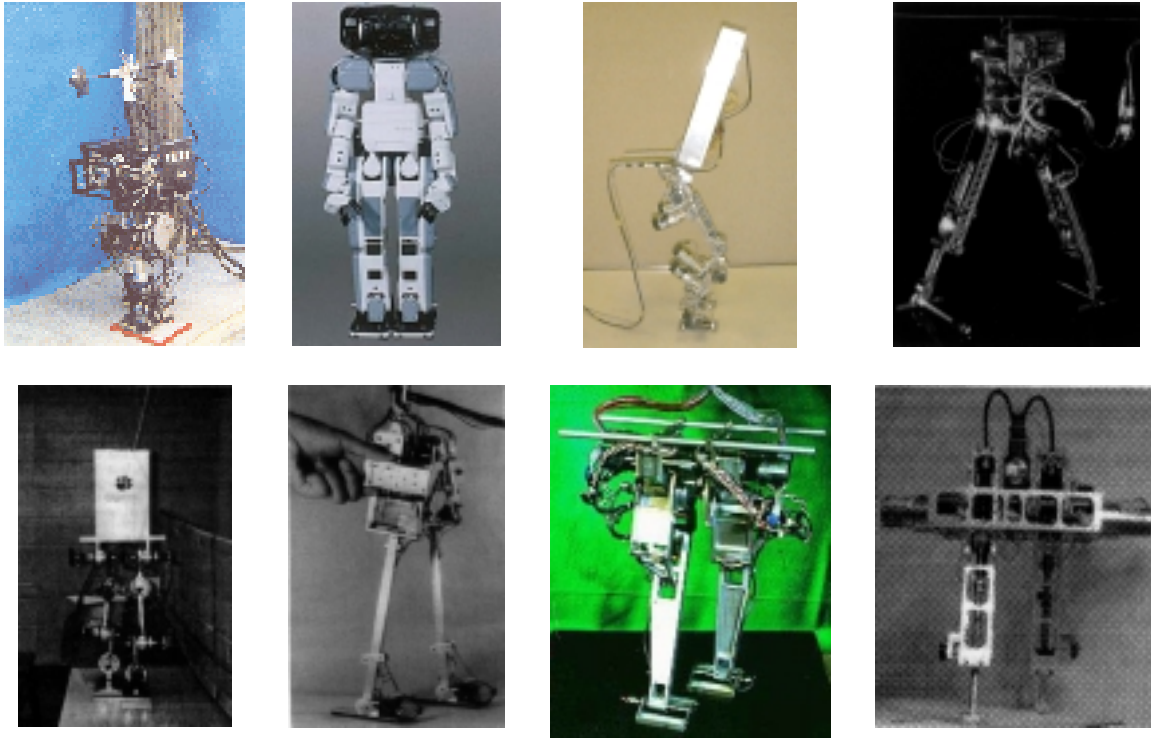


Figure 3-1: Some previous powered bipedal walking robots. From top left to bottom right are WL-10RV1 from Waseda, P2 from Honda, Toddler from UNH, the Moscow State University Biped, SD-2 from Clemson and Ohio State, Biper from University of Tokyo, Meltran II from Mechanical Engineering Lab in Tsukuba, and Timmy from Harvard. Figures compiled by J. Pratt.

3.3 Powered Bipedal Walkers

Many bipedal walking robots have been built over the years. Several of these robots are shown in Figure 3-1. These biped walking robots fall into two broad categories: those which predominantly use pre-recorded trajectory playback and those which predominantly use an algorithmic controller. All the robots employ a high impedance actuation scheme and none take advantage of natural dynamics.

Passive dynamics were successfully implemented in actuated robots as well. J. Pratt (16) developed algorithms that used the natural dynamics of the swing leg to efficiently control a planar bipedal robot. More recently, J. Pratt has developed three-dimensional simulations of M2 using passive elements such as a knee cap, a compliant ankle, and a passive swing leg to achieve natural looking and efficient walking.

3.4 Series Elastic Actuators

Series Elastic Actuators(SEA's)(14) are actuators which have an elastic element in series with the motor and gear train. A sensor measures the displacement of the elastic element and force is implied by Hooke's Law, $F = kx$. In short, SEA's provide force control, shock tolerance, and low impedance actuation. A more detailed account of their benefits and limits can be found in Robinson et al.(17)

A rendering of the SEA used on M2 can be seen in Figure 3-2. The brushless DC motor is modified to have a ballscrew as its rotor. The output of the ballscrew is attached to an aluminum

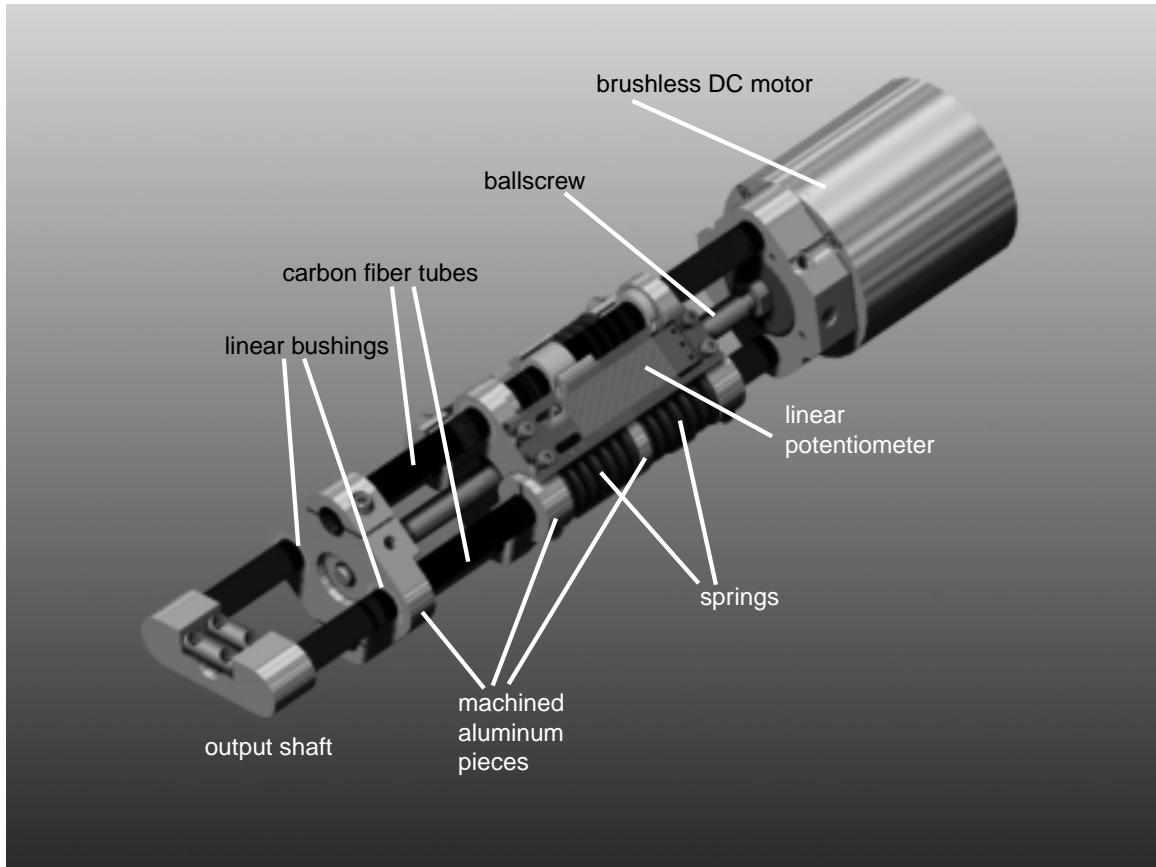


Figure 3-2: An annotated rendering of the Series Elastic Actuator which is used in the robot M2. Modeled and rendered by David Robinson.

piece which is sandwiched between a set of linear compression springs. The other ends of the springs are attached to the output of the actuator. A linear potentiometer measures the ballscrew displacement with respect to the output shaft, thereby measuring the spring compression and giving an indication of the force output.

On the specific SEA designed for M2(17), a simple analog PD controller is implemented to control the spring deflection. When the output of the actuator is clamped, a force control bandwidth of 30hz is observed. The actuator is capable of outputting 300 lbs and capable of resolving forces on the order of 1.5 lbs.

Chapter 4

Robot Mechanical Design

This chapter presents the design specifics of the bipedal robot M2.

4.1 General Robot Architecture

The robot stands approximately 5 feet high and weighs 60 pounds. The robot has 12 active degrees of freedom. Table 4.1 lists the specifications for the joints of the robot. Power at each joint is the same due to the single actuator design employed for all the joints. The power to the individual degrees of freedom of the ankle joint is limited by the power of the other.

The robot joint ranges of motion were chosen based on data from humans as well as the robot Spring Flamingo and preliminary dynamic computer simulations.

4.2 The Design

4.2.1 Overall Structure

A photo of the robot and a joint schematic view are shown in Figure 4-1. The leg of the robot has six active degrees of freedom plus an optional passive degree of freedom in the foot. The vertical axis, Z , is the yaw axis. The X axis is the roll axis and the Y axis is the pitch axis. The hip has three degrees of freedom. These three degrees of freedom are made up of a universal joint (yaw and roll) followed by a pin joint (pitch). The pitch pin joint is offset slightly (about 2cm) from the yaw and roll axes.

The frontal plane dimensions of the robot are shown in Figure 4-2. The dimensions are very close to the dimensions for a 50th percentile US male as given by Whitney(2). The ranges of motion are adapted from robot simulations and data found in Rose, et al.(18), Winter(20), and Kapandji(7).

	deg	rad/s	Nm	Drive Type
hip(pitch)	80,-30	7.3333	50	Pulley
hip(roll)	30,-20	6.8	59	Push-rod
hip(yaw)	30,-15	5.5	67	Push-rod
knee(pitch)	80,0	8.8	42	Push-rod
ankle(pitch)	45,-20	8.8	88*	Push-rod
ankle(roll)	20,-20	7.3	100*	Push-rod

Table 4.1: Robot Joint Specifications. Torque and rad/s numbers are given for maximum moment arm. Power, torque, and velocity are symmetric due to the actuator. *The ankle roll and pitch are not independent. Their maximum values can not be applied simultaneously.

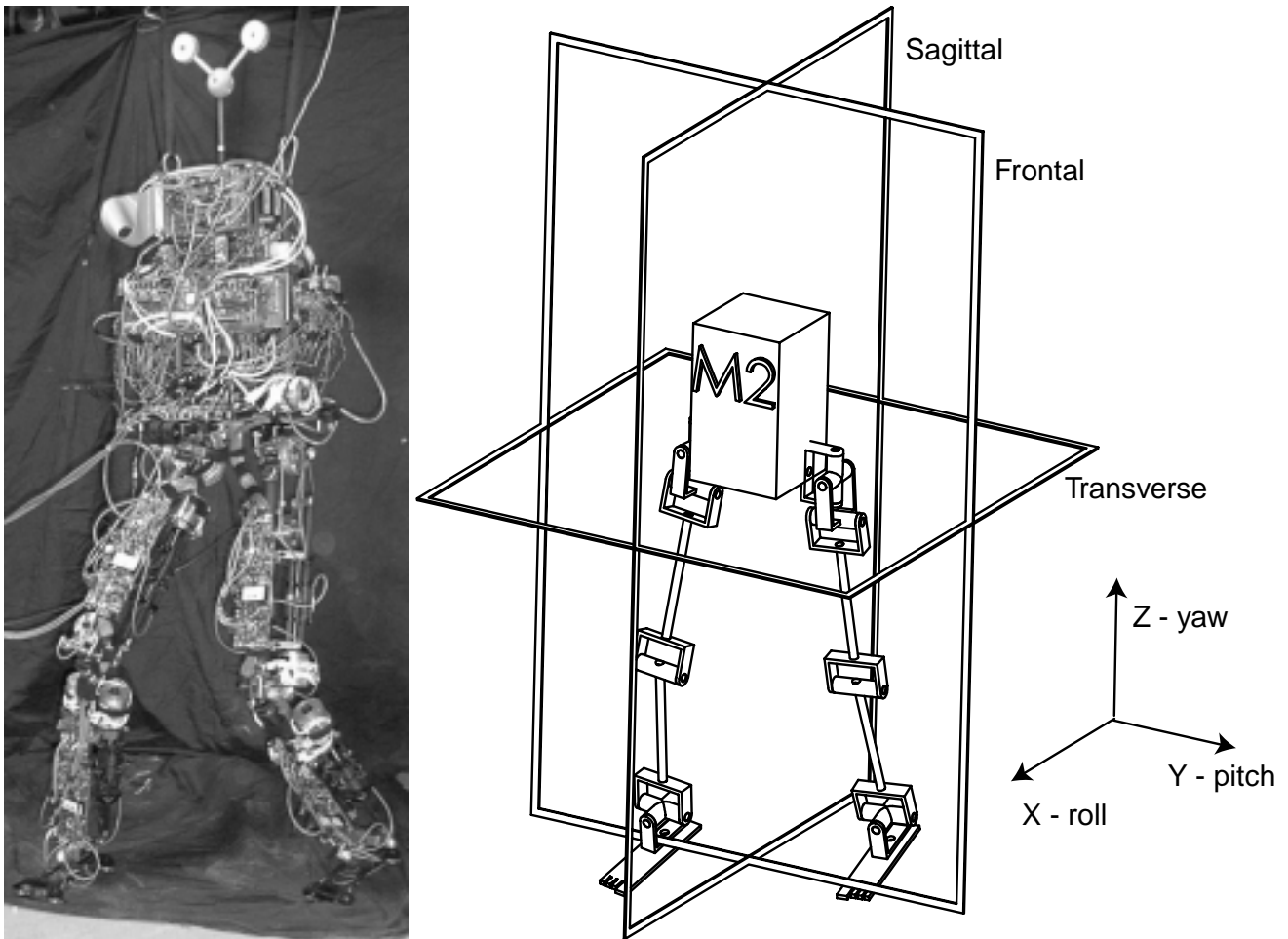


Figure 4-1: A photo of the completed robot and a joint schematic view of the robot. The schematic shows active degrees of freedom only. The optional passive toe joint is not shown.

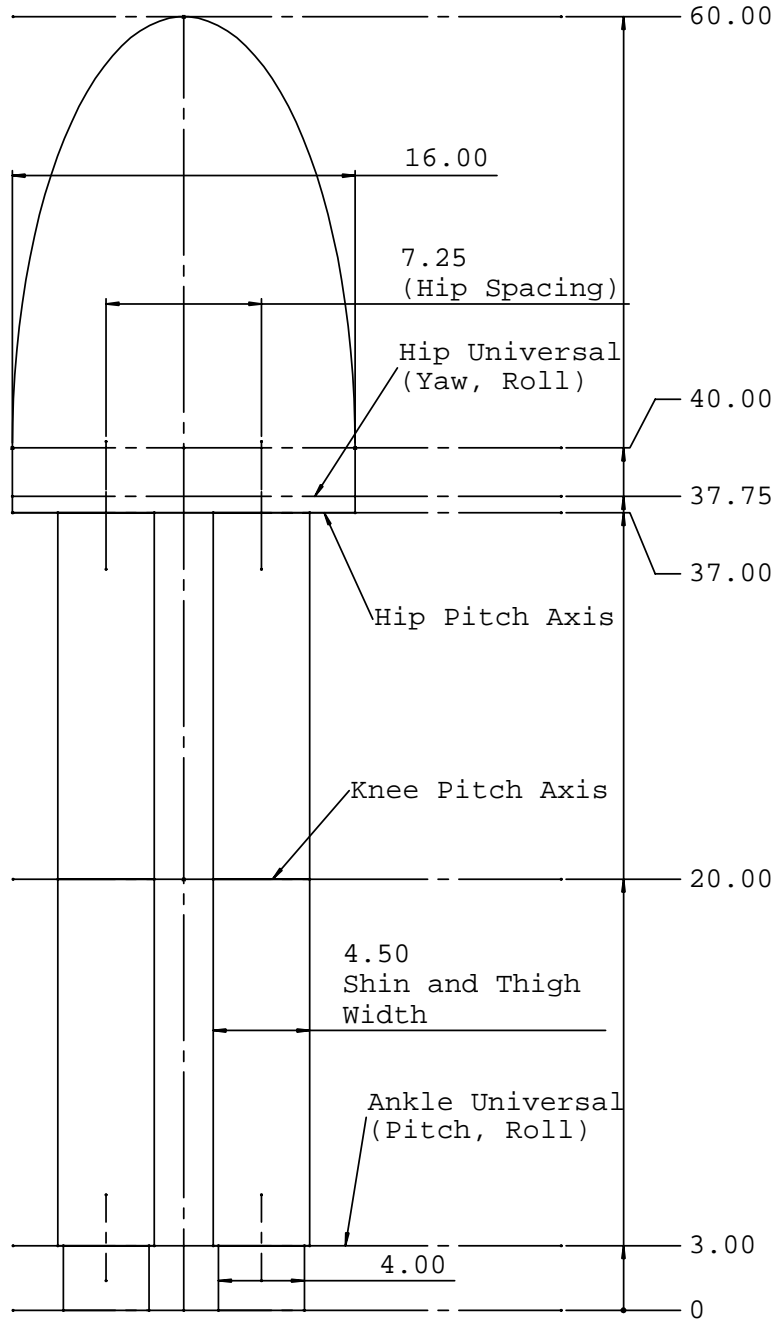


Figure 4-2: The dimensions of the biped in the frontal plane. The body and links are approximately axially symmetric about their longitudinal axis. Dimensions are in inches.

Body Part/Area	Human	Biped Robot	PDW
Shin & Foot (x2)	6%	13.5%	10%
Thigh (x2)	10%	11%	15%
Ab/Pelvic	27%	51 %	50%
Arm (x2)	5%	NA	NA
Thorax to Head	31%	NA	NA

Table 4.2: Approximate distribution of mass in humans, the biped M2, and McGeer’s kneed passive dynamic walker(PDW). Human data adapted from Dempster and Gaughran (3). Robot weight distribution is driven primarily by actuator locations. Each actuator is approximately 1.2kg(2.5 lbs).

The mass distribution of the robot is dominated by the location of the actuators within the links. As a result, the robot’s mass distribution is centered lower than an average human’s. Table 4.2 shows the percentage mass distributions for an average male, M2, and a planar passive dynamic walker(10). The robot mass distribution is closer to that of a planar passive dynamic walker than to that of a human. Due to successful computer simulations(16), it was not necessary to add additional weight to the torso in order to put the proportions more in line with a human.

4.2.2 Actuators

The actuators used in the robot are 90W, 1.2KG Series Elastic Actuators(17). They are capable of a maximum force of roughly 1320N (300lbs) and a maximum speed of roughly 0.28 m/s (11 in/s). The actuators have a force control bandwidth of 30Hz. Linear actuators were chosen over rotary actuators due to the available space in the robot. Linear actuators allowed for placement along the longitudinal axis of the leg links. The actuators are symmetric in their power, speed, and force capabilities.

4.2.3 Ankle

The ankle of the biped is a universal joint. The pitch axis is followed by the roll axis. This is a slight deviation from the structure of the human ankle. The human ankle is often likened to a universal joint where the second axis is at 45 degrees to the first rather than at 90 degrees(7). For engineering simplicity we use a universal joint with orthogonal axes. The instantaneous power requirement for ankle pitch is the greatest. The actuators were placed in a configuration so they can act together in the pitch direction.

Photos of the ankle are shown in Figure 4-7 and a schematic of the ankle and its actuators are shown in Figure 4-3. The ankle has two series elastic actuators placed along the longitudinal axis of the shin. The actuators are mounted by a universal joint near the top of the shin and attached to the foot by a ball and socket joint (rod-end). This is a linkage variation of a standard geared differential. When the actuators push in unison, a moment is generated about the pitch axis. When they push in opposite directions, a roll moment is generated.

4.2.4 Foot

Two different feet were designed for the robot. One foot is a simple rectangular design with four single axis load cells residing at each of the corners. This foot closely resembles the foot that was used in computer simulations in the lab. Another more involved foot was designed in order to explore the roll of the toes in walking.

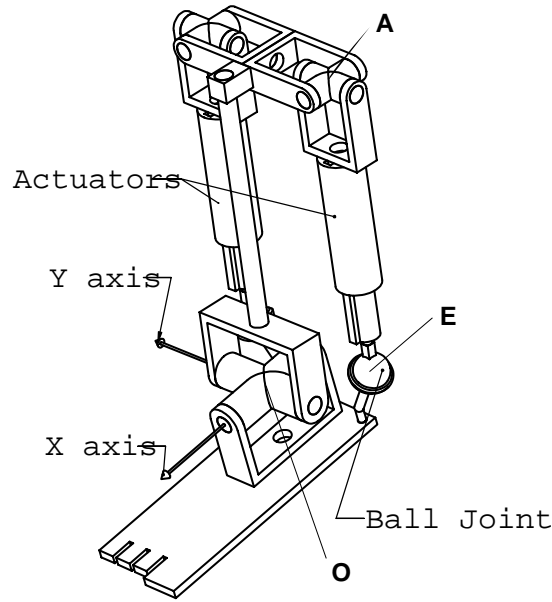


Figure 4-3: A schematic of the ankle joint actuation scheme. The axes shown are fixed to the center of the universal joint. The points A,E, and O are referenced in Appendix A.

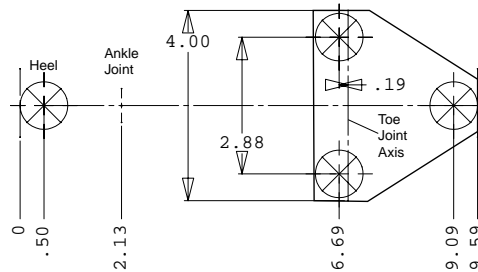


Figure 4-4: The dimensions of the biped foot with passive toe joint. The X's represent the location of the load cells.

The more intricate second foot of the biped robot contains a passive joint which is modeled after the toe of a human. The joint is believed to smooth the center of mass trajectory of the body during a walking cycle(18). The toe joint is simply a pin joint with two limit stops and a soft return spring.

Ground contact and sensing on the foot consists of four single axis load cells. One cell is placed at the heel and three cells are placed in a triangle at the toe/ball of the foot. The three cells in the toe are all constrained to the same plane. The three toe contact points can rotate about the foot Y-axis with respect to the heel contact point. The layout of the sensors can be seen in Figure 4-4.

Standard through-hole button load cells are used. There is a rubber bumper which contacts the ground roughly 0.875" in diameter attached to each load cell. On the simple four point foot there is a rectangular pastic piece with a 0.25" piece of neoprene for grip and shock absorbtion. This can be seen in Figure 4-7. Single axis load cells were chosen over a six axis sensor because of their size and weight, and chosen over strain gauges because of their ease of use and quick replaceability.

On the more complicated biped foot, force control and a passive toe joint are the reasons the four contact points of the foot are not over-constrained. Since ankle roll is force controlled rather than position controlled, it can adjust itself so the three points of the toe lie flat. The passive toe

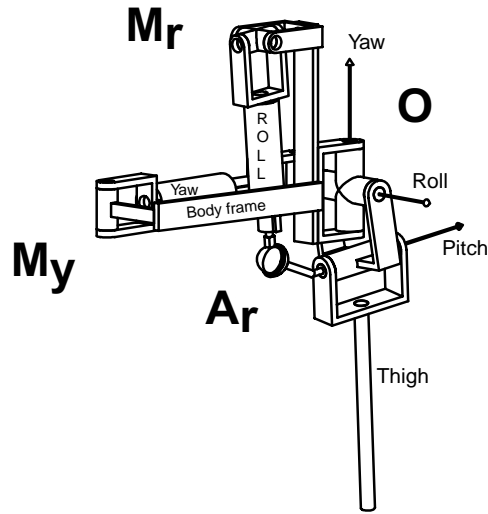


Figure 4-5: A schematic of the biped hip. The pitch actuator is not shown. It lies along the axis of the thigh.

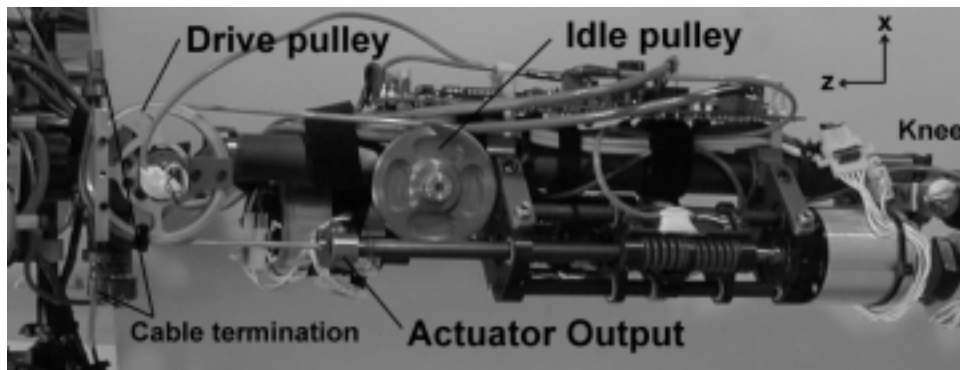


Figure 4-6: A photo of the biped thigh illustrating the hip pitch cable drive system.

joint(a pitch joint) then allows the fourth point on the heel to lie flat as well.

4.2.5 Hip

The biped hip has three degrees of freedom. The joint consists of a universal joint followed by a slightly offset pin joint. A schematic of the hip is shown in Figure 4-5. The yaw axis is first and the yaw actuator is mounted to the body frame with a pin joint. The roll actuator is next. Since its attachment point passes through the roll angle, it is mounted to the body by a universal joint. Its endpoint is attached by a ball and socket joint. The pitch actuator, which is not shown, lies along the longitudinal axis of the thigh. It is the only actuator which is attached using a cable and pulley rather than a rod-end. The range of motion of the hip pitch joint is the largest. The moment arm changes associated with a drive arm would be too great at the extents of the pitch motion. At sixty degrees from the perpendicular drive position, the moment arm would be half its original length.

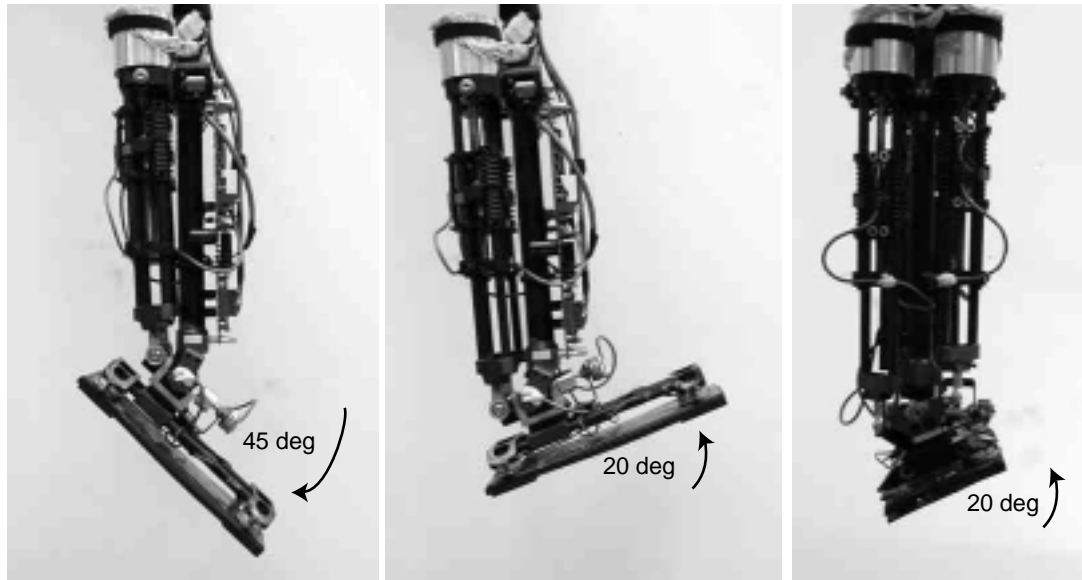


Figure 4-7: The ranges of motion on the robot ankle joint. The ankle roll is symmetric(± 20 deg).

4.2.6 Knee

The robot knee is a simple pin joint. The joint is actuated by a SEA located in the thigh. Two photos demonstrating the range of motion of the knee can be seen in Figure 4-8.

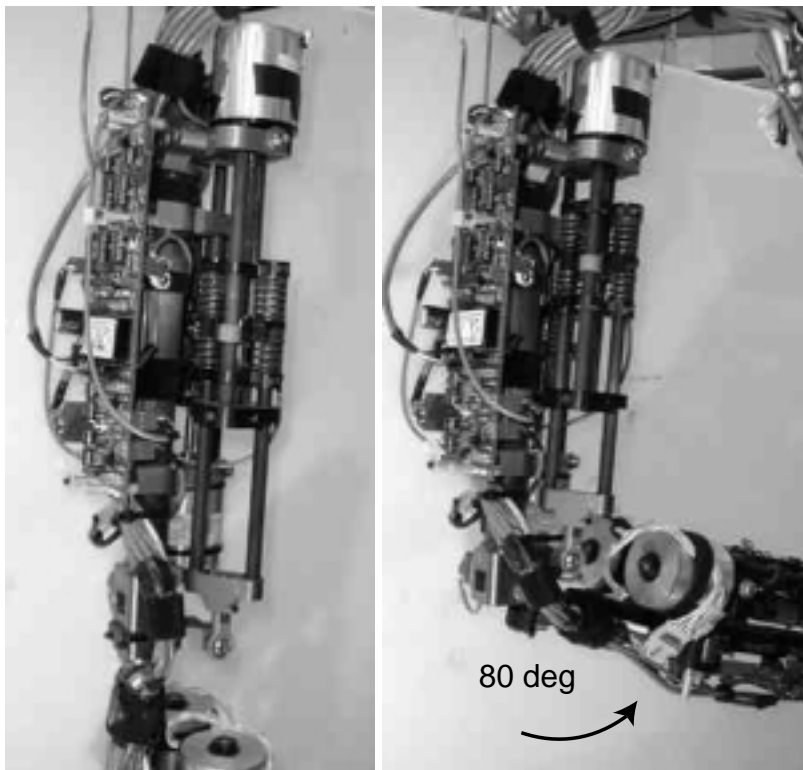


Figure 4-8: The range of motion of the robot knee. The knee has 80 degrees of motion.

Chapter 5

Electronics and Control Systems

5.1 Electronics Overview

The basic electronic subsystems of the robot are shown in Figure 5-1. The robot is powered by a 48 Volt power supply. There is also an Ethernet connection not shown in the figure which can be used to load control code and retrieve data from the on-board computer. The circuit boards are summarized in Table 5.1. The sensors are summarized in Table 5.2.

All signals are sent and received differentially between the computer and the analog boards.

5.1.1 48 Volt bus

All the electronics on the robot receive power from a 48 Volt bus. The current setup has the robot connected to several offboard 48V power supplies. All the electronics were designed with this power bus in mind. The voltage choice was dictated by the brushless motor amplifiers. It was also chosen because it is a standard voltage and the robot will eventually be augmented with batteries for future autonomous demos.

5.1.2 Robot Sensors

The robot is equipped with a total of 33 sensors. There are 12 rotary potentiometers that are used to measure joint position and this is differentiated to give the joint velocity. The joint position measurements are relative displacements between joints. There are 12 linear potentiometers which measure the spring compression in the Series Elastic Actuators. These signals are local to the analog force control loop only. They are not used by the DSP in the control. There are 8 single axis load cells on the feet of the robot. These sensors are connected to the strain gauge conditioning board which amplifies and buffers the signal on its way to the DSP. There is a single Intersense Inertia

Table 5.1: Circuit Boards on the Robot

	QTY	Voltage Input	Vendor
Motor Amplifiers	12	+48	Copley Controls
DSP	1	+5	Dideas
ANA074	1	5,12	Dideas
ANA063	1	5,12	Dideas
Analog Force Control Board	6	+48	Leg Lab
Power Distribution Board	2	+48	Leg Lab
Signal Conditioning Board	4	12	Leg Lab
IS-300 Signal Conditioner	1	+12	Intersense

Table 5.2: Sensors on the Robot

Sensor	QTY	Voltage Input	Vendor
Rotary Potentiometers	12	+5	Bourns
Linear Potentiometers	12	+5	Novotechnik
Single-Axis Load Cells	8	+9	Transducer Techniques
3-axis inclinometer	1	NA	Intersense

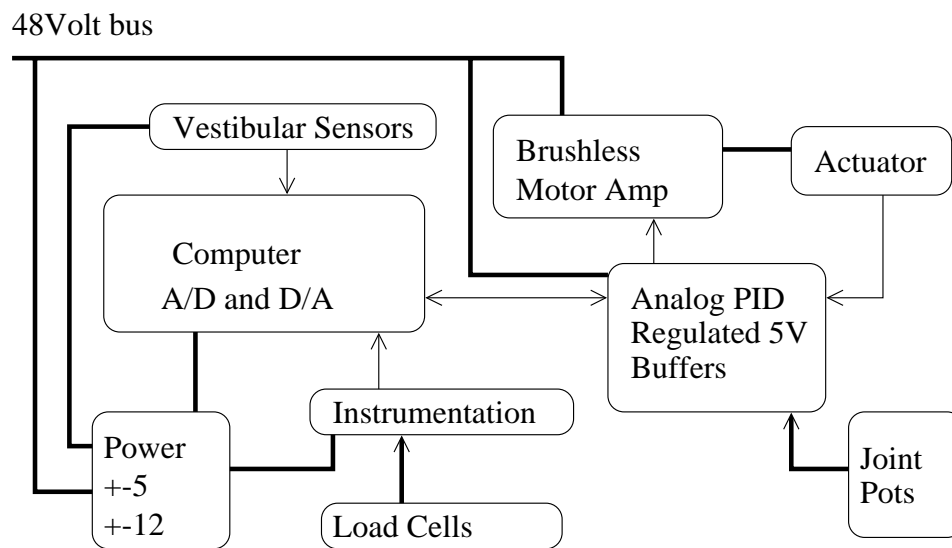


Figure 5-1: An overview of the biped electronics. Thick lines indicate power transfer and arrowheads indicate information flow.

Cube™ which measure the roll, pitch, and yaw(magnetic) of the robot body. The Inertia Cube is connected to a IS-300 motion tracker unit which communicates with the DSP through a RS-232 serial line. Table 5.2 provides a summary of the robot sensors. Figure 5-2 contains an annotated photo of M2 with the sensor locations.

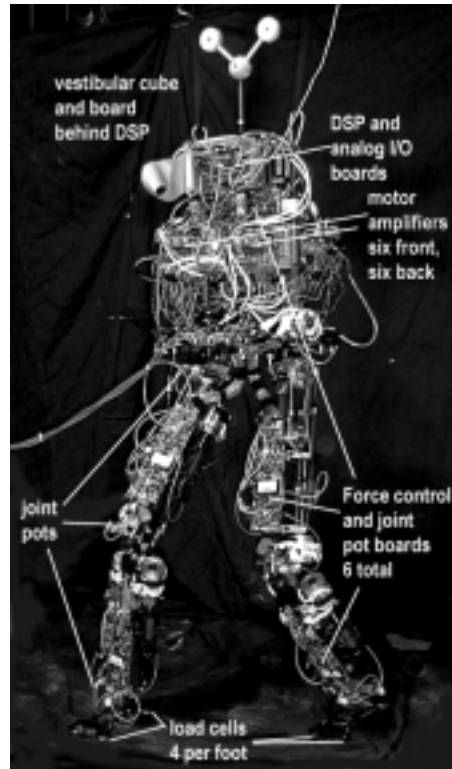


Figure 5-2: A photo of M2 with annotations of electrical systems.

5.2 Custom Circuit Boards

5.2.1 The Signal Conditioning Boards

The signal conditioning boards are four layer printed circuit boards. They have a ground plane, a power plane, and two routing layers. The signal conditioning boards handle two 350 ohm wheatstone bridge sensors each. They have adjustable gain and offsets.

5.2.2 The Analog Force Control Boards

The analog force control board provides two channels of PID force control for the Series Elastic Actuators and two channels of joint potentiometer buffering and differentiation. The analog force control boards have a 48 Volt power input and communicate with the DSP through differential amplifiers and receivers.

The analog force control boards are four layer printed circuit boards. They have a ground plane, a power plane, and two routing layers.

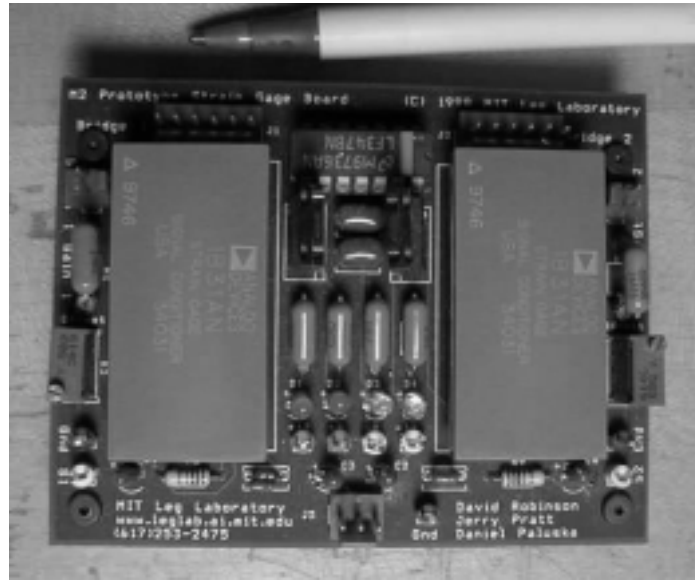


Figure 5-3: A photo of the biped strain gauge signal conditioning board. This board handles two strain gauges. There are a total of four of these boards on the robot.

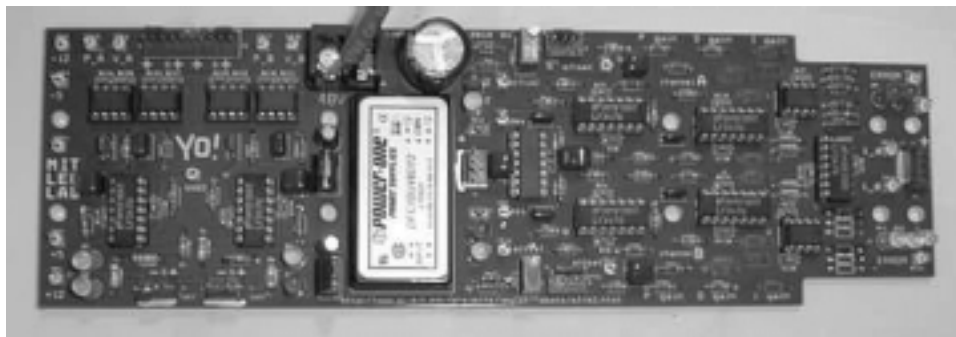


Figure 5-4: A photo of the analog force control and joint pot buffer board. There are six identical boards on the robot.

5.2.3 The Analog Breakout Board

The analog breakout board connects to the ANA070 and ANA064 analog input and output boards. It has no power and simply allows for the use of smaller connectors to easily distribute the 64 channels of analog input and output from the ANA070 and ANA064 boards. There are two 64 pin connectors which connect to the ANA064 and ANA070 boards respectively. Then there are multiple 3,5, and 10 pin connectors which connect to the signal conditioning boards and analog force control boards. The analog breakout board is a two layer printed circuit board.

5.2.4 The Power Distribution Boards

The power distribution board has a 48 Volt input and outputs a variety of lower voltages. It appears in two places on the robot. There is one printed circuit for the two power distribution boards but there are two different DC-to-DC converters which are used when assembling the board.

- **Board Configuration 1** This board supplies power to the DSP (+5V) and two analog boards (+12V, +5V). The analog and digital grounds are isolated.
- **Board Configuration 2** This board provides power to the Intersense IS-300(+12V) and the four signal conditioning boards (+12V).

The power distribution boards are four layer printed circuit boards. They have a ground plane, a power plane, and two routing layers.

5.2.5 The DSP and Analog I/O

M2 has a custom DSP system that was designed by Chris Barnhart at Digital Designs and Systems. The DSP is a Texas Instruments C-31. There are three circuit boards that make up the system.

1. DSP. Multiple Serial Lines and Digital I/O.
2. 16 Analog Ins, 16 Analog Outs, and Ethernet.
3. 32 Analog Inputs.

5.3 Control Software

Control code for the robot is written in C. It is compiled offline on a Unix machine and downloaded to the robot via Ethernet. The main robot control code runs at 500Hz on the DSP and sends desired forces to the analog boards. Currently, the control system treats the actuator and analog boards as a 'black box' force source. This means it is assumed that the desired force sent out to the actuator is the actual force applied to the joint. This is true within the realm of frequencies needed for walking (less than 15Hz). The analog boards have PD control loops for the Series Elastic Actuators. The analog boards also buffer and differentiate the joint potentiometers and send the information to the DSP.

This is similar to the electronics used for Spring Flamingo. The main differences are the addition of Ethernet for faster communication with the outside world and differential send and receive for signals within the robot.

Bibliography

- [1] Jesper Adolfsson, Harry Dankowicz, and Arne Nordmark. 3-d stable gait in passive bipedal mechanisms. Proceedings of 357 Euromech, 1998.
- [2] Henry Dreyfus Associates. The Measure of Man and Woman. Whitney Library of Design, New York, 1993.
- [3] W.T. Dempster and G. Gaughran. Properties of body segments based on size and weight. American Journal of Anatomy, 1965.
- [4] J. Fowble and A. Kuo. Stability and control of passive locomotion in 3d. Proceedings of the Conference on Biomechanics and Neural Control of Movement, pages 28–29, 1996.
- [5] Mariano Garcia, Anindya Chatterjee, and Andy Ruina. Speed, efficiency, and stability of small-slope 2d passive dynamic bipedal walking. IEEE International Conference on Robotics and Automation, pages 2351–2356, 1998.
- [6] K. Hirai, M. Hirose, Y. Haikawa, and T. Takenaka. The development of honda humanoid robot. IEEE International Conference on Robotics and Automation, 1998.
- [7] Ibrahim Adalbert Kapanji. The Physiology of the Joints. Churchill Livingstone, 1982.
- [8] Benjamin Krupp. Design and control of a planar robot to study quadrupedal locomotion. Master’s thesis, Massachusetts Institute of Technology, August 2000.
- [9] Tad McGeer. Passive dynamic walking. International Journal of Robotics Research, 9(2):62–82, 1990.
- [10] Tad McGeer. Passive dynamic biped catalogue. Proceedings of the 2nd International Symposium of Experimental Robotics, 1991.
- [11] Thomas A. McMahon. Mechanics of locomotion. The International Journal of Robotics Research, 3(2):4–28, 1984.
- [12] Gill A. Pratt and Matthew M. Williamson. Series elastic actuators. IEEE International Conference on Intelligent Robots and Systems, 1:399–406, 1995.
- [13] J. Pratt, P. Dilworth, and G. Pratt. Virtual model control of a bipedal walking robot. IEEE International Conference on Robotics and Automation, pages 193–198, 1997.
- [14] Jerry E. Pratt. Virtual model control of a biped walking robot. Master’s thesis, Massachusetts Institute of Technology, August 1995.
- [15] Jerry E. Pratt and Gill A. Pratt. Exploiting natural dynamics in the control of a planar bipedal walking robot. Proceedings of the Thirty-Sixth Annual Allerton Conference on Communication, Control, and Computing, pages 739–748, 1998.
- [16] Jerry E. Pratt and Gill A. Pratt. Exploiting natural dynamics in the control of a 3d bipedal walking simulation. Proceedings of the International Conference on Climbing and Walking Robots (CLAWAR99), 1999.

- [17] David W. Robinson, Jerry E. Pratt, Daniel J. Paluska, and Gill A. Pratt. Series elastic actuator development for a biomimetic robot. IEEE/ASME International Conference on Advanced Intelligent Mechatronics, 1999.
- [18] Jessica Rose and James G. Gamble. Human Walking. Williams and Wilkins, 1994.
- [19] Mark Roshier. Robot Wrist Actuators. John Wiley and Sons, Inc., 1989.
- [20] D. A. Winter. Biomechanics and Motor Control of Human Movement. John Wiley and Sons, Inc., New York, 1990.
- [21] Jinichi Yamaguchi, Eiji Soga, Sadatoshi Inoue, and Atsuo Takanishi. Development of a bipedal humanoid robot - control method of whole body cooperative dynamic biped walking. IEEE International Conference on Robotics and Automation, pages 368–374, 1999.

Appendix A

Joint Math

Since all of M2's rotary joints are actuated by linear actuators, transformations are needed to get from joint torques to actuator forces. These are dependent upon the joint layout and actuation scheme. If the force is known, the torque is somewhat easily computed using the formula, $\tau = \vec{r} \times \vec{F}$.

The cross product $\tau = \vec{r} \times \vec{F}$ operation can be rewritten as a matrix multiplication $\tau = A\vec{F}$ where A is a singular matrix.

$$\tau = \vec{r} \times \vec{F} = \begin{vmatrix} i & j & k \\ r_1 & r_2 & r_3 \\ F_1 & F_2 & F_3 \end{vmatrix} = \begin{bmatrix} 0 & -r_3 & r_2 \\ r_3 & 0 & -r_1 \\ -r_2 & r_1 & 0 \end{bmatrix} \vec{F} = A\vec{F} \quad (\text{A.1})$$

However, if the cross-product is written as $\tau = |\vec{R}||\vec{F}|\sin(\theta)$ then we can easily invert. In the case of most of the robot joints, this requires use of the arctan function or the law of cosines to find the angle θ . In general, the direction of \vec{F} is fixed by the geometry of the joint and $|\vec{F}|$ is the quantity of real interest.

A.1 Knee Joint

The knee joint is a single degree of freedom rotary joint allowing relative motion between the shin and the thigh. When all the joints of the robot are zero(it is standing with locked knees), the knee axis is parallel to the global Y axis. Rotation about the knee joint is referred to as pitch.

The knee actuator is connected to the knee joint via a push rod of length $|\vec{OA}| = r_k$ at the shin and a fixed pin joint at the thigh.

The knee joint has three points of interest which we will use for the derivation of the transformation. The knee pivot O , the actuator pushrod attachment A , and the actuator mounting pivot M . The robot knee joint and points can be seen in Figure A-1 and a simple line drawing is seen in Figure A-2.

$$\tau = \vec{r} \times \vec{F} = r_k \sin(\angle OAM) F_{knee} \quad (\text{A.2})$$

The actuator force required given τ_k is

$$F_{knee} = \frac{\tau_k}{r_k \sin(\angle OAM)} \quad (\text{A.3})$$

where F_{knee} is a scalar and $\angle OAM$ can be defined as follows

$$\angle OAM = \theta_{fixed} + \theta_k - \angle AM = \theta_{fixed} + \theta_k - \arctan \frac{r \sin(\theta_{fixed} + \theta_k) - L_2}{L_1 + r \sin(\theta_{fixed} + \theta_k)} \quad (\text{A.4})$$

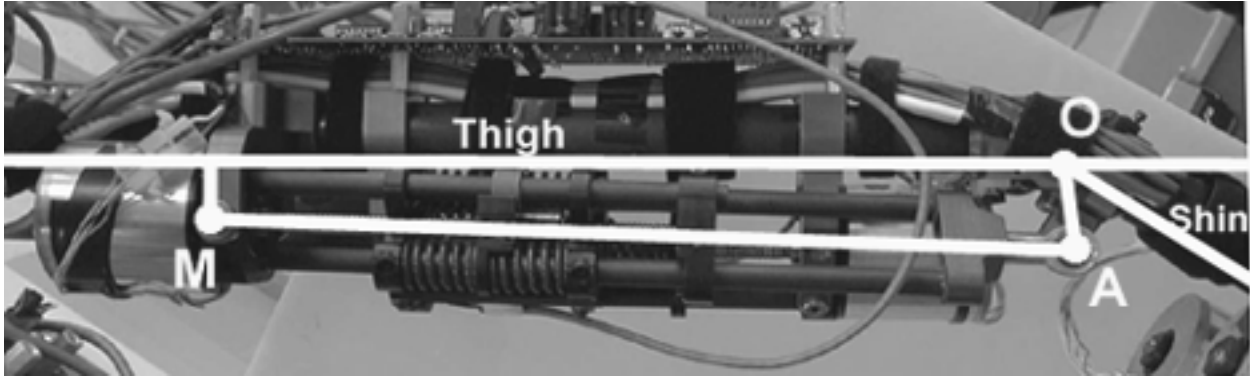


Figure A-1: The robot knee joint with superimposed lines and points. Points O, A and M all refer to pin joints. O is the knee joint. M is where the actuator is mounted to the thigh and A is where the actuator is attached to the shin.

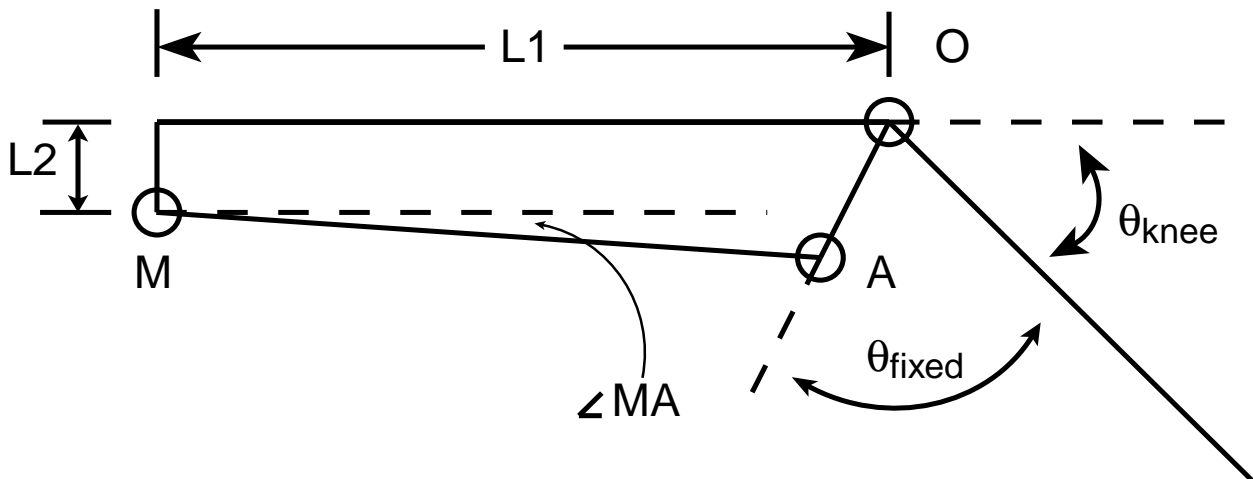


Figure A-2: A line drawing of the knee for the calculation of knee actuator desired force. The actuator is the line segment \vec{MA} . This drawing also pertains to the geometry of the hip and ankle joints but the hip and ankle actuators have motions out of the plane whereas the knee actuator is always in the plane perpendicular to the knee axis.

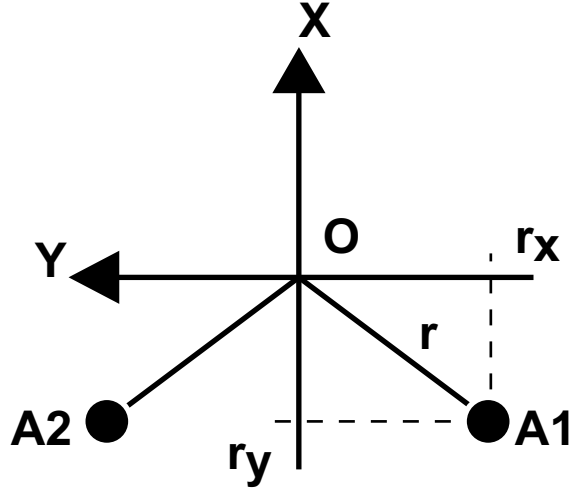


Figure A-3: A simple view of the actuation of the robot ankle. This is a tranverse plane slice of the robot ankle. Point O is the intersection of the X and Y axes as well as the center of the ankle universal joint. Points A1 and A2 represent the attachment points of the two actuators respectively. Forces in the actuators create torques about both the X and Y axes. Joint rotations change the relative lengths of the X and Y projections(r_x and r_y) of the moment arms, therefore affecting the torque to force transformation.

The angle between the shin and the thigh is θ_k and the constant, θ_{fixed} , is the angle between the shin and the segment \vec{OA} . It is also possible to derive the equations avoiding the inverse tangent by using the law of cosines.

It would be possible to simplify the equations a bit by assuming the actuator is always parallel to the thigh, i.e. $\angle \vec{AM} = 0$. This simplifies the equations and shouldn't reduce accuracy much considering that $L_1 \gg L_2$. Equation A.3 then becomes

$$F_{knee} = \frac{\tau_k}{r_k \sin(\theta_{fixed} + \theta_k)} \quad (\text{A.5})$$

where F_{knee} is once again a scalar quantity.

A.2 Ankle Joint

The ankle joint is a universal joint(2 d.o.f.) allowing relative motion between the foot and the shin. When all of the joints of the robot are zero, the axes of the ankle joint line up with the global X and Y axes. The Y axis is proximal to the shin. Rotation about the Y axis is referred to as pitch and rotation about the X axis is referred to as roll. The math for the ankle is an extension of the math for the knee.

We can consider the ankle as two decoupled cases of the knee joint. Then one can simply add the forces from τ_{aroll} and τ_{apitch} . There is a slightly more complicated analogy to the knee in two planes of the ankle. The ankle roll considers what is happening in the XZ plane and the ankle pitch considers what is happening in the YZ plane. Both planes are coming out of the page in Figure A-3. Each plane looks similar to the knee diagram shown in Figure A-2. The main difference is that $|OA| = r$ is a function of the other ankle angle.

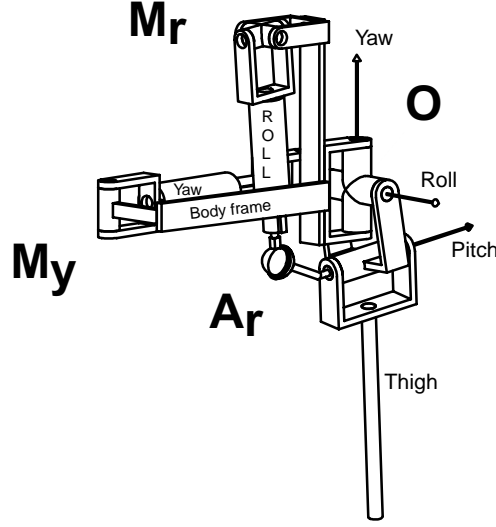


Figure A-4: The robot hip joint schematic. Point O refers to the hip universal joint. The Z(hip yaw) and Y(hip roll) axes intersect at point O . Point M_r refers to the universal joint on the body where the roll actuator is mounted. Point A_r refers to the ball joint on the thigh where the roll actuator is attached. Point M_y refers to the pin joint where the yaw actuator is attached to body. Point A_y is the pin joint attachment of the yaw actuator to the yaw universal block. It is hidden in this schematic.

A.3 Hip Joint

A.3.1 Hip Pitch

The math for the hip pitch is the simplest of all the joints since the hip pitch actuator is attached by a pulley. The desired torque at the joint(τ_{hp}), leads to the force(f_{hp}) command to the hip pitch linear actuator.

$$f_{hp} = \frac{\tau_{hp}}{r_{hippitch}} \quad (\text{A.6})$$

The transformation from actuator velocity to joint velocity is quite simple as well.

$$\omega_{hp} = \frac{vel_{hp}}{2\pi r_{hp}} \quad (\text{A.7})$$

A.3.2 Hip Roll and Yaw

The yaw actuator transformation is identical to that of the knee actuator except for the addition of a small term which can be ignored with little affect.

The actuator force required given τ_{hyaw} is

$$F_{hyaw} = \frac{\tau_{hyaw}}{\sin(\angle O_y A_y M_y)} + \epsilon_{hroll} \quad (\text{A.8})$$

where ϵ is a small factor due to the torque applied to hip roll which is a function of the hip roll and yaw angles. O_y , A_y , and M_y are defined as they were in the case of the knee.

The actuator force required given τ_{hroll} can be simplified to

$$F_{hroll} = \frac{\tau_{hroll}}{\sin(\angle O_{hr}A_{hr}M_{hr})}(1 + \epsilon_{hyaw}) \quad (\text{A.9})$$

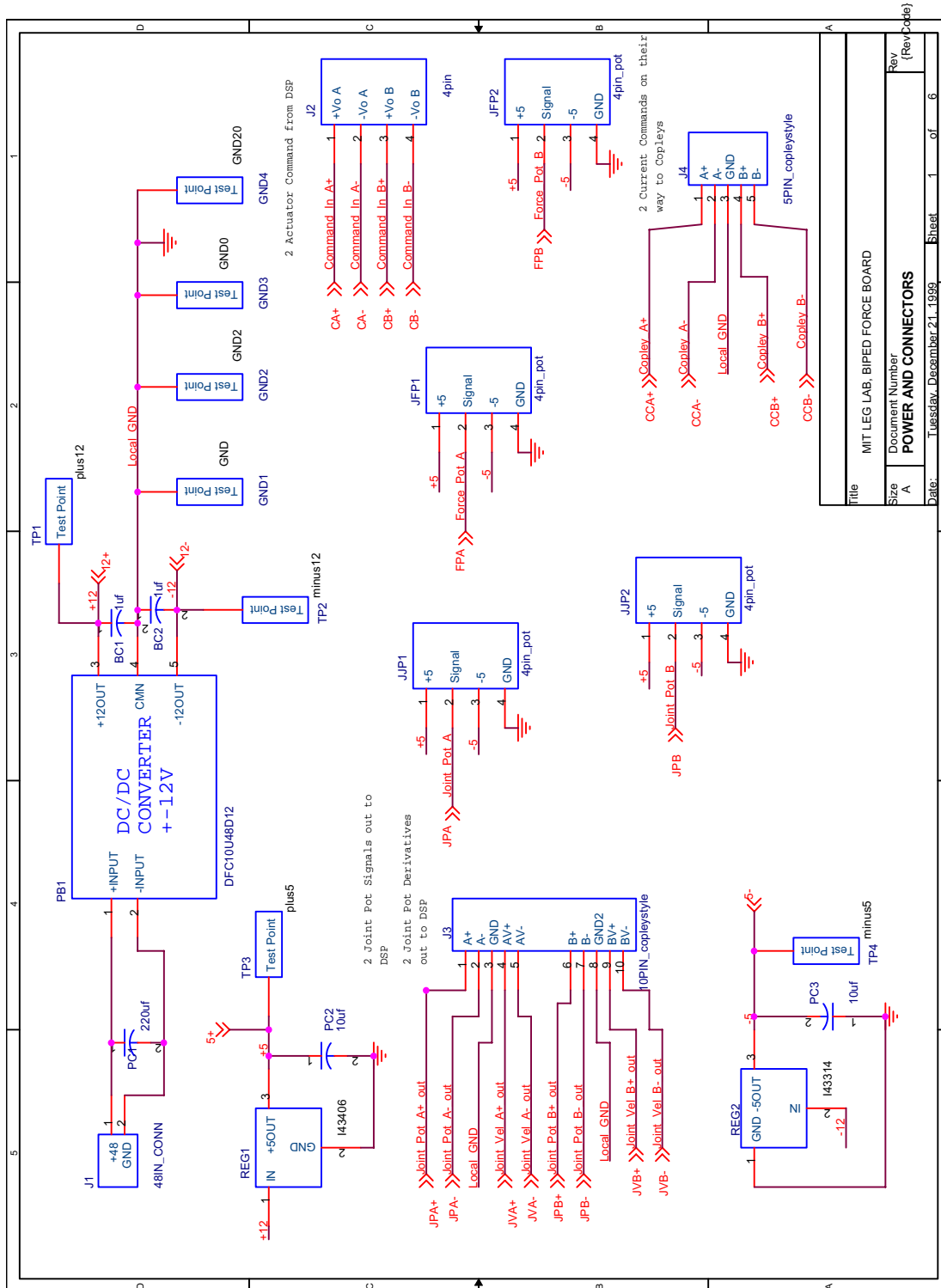
The exact equation for the hip roll incorporates the yaw angle. Since the hip roll actuator attachment point A_{hr} is attached to the leg below the yaw degree of freedom, the points O_{hr} , A_{hr} , and M_{hr} do not always lie within the plane perpendicular to the roll axis as in the case of the knee joint where they are fixed in the plane perpendicular to the knee axis.

When the roll actuation plane(plane formed by the three points O_{hr} , A_{hr} , M_{hr}) is skewed with respect to the roll axis, a small torque will be contributed to the yaw axis. This is where the term ϵ_{hroll} comes from in Equation A.8 and this is why the hip roll equation has the ϵ_{hyaw} term in it.

Appendix B

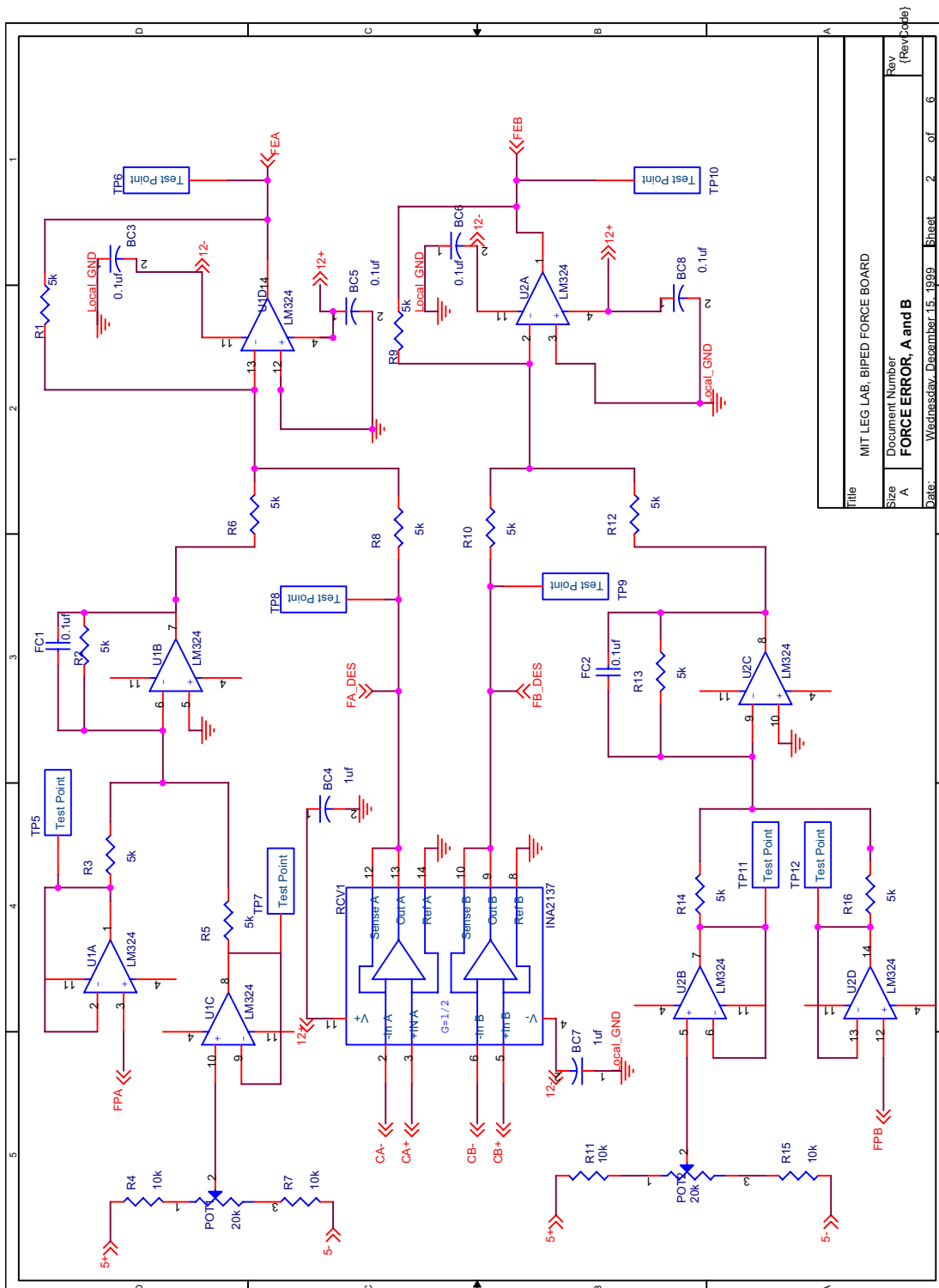
Electrical Schematics

This Appendix contains the electrical schematics for all the custom circuit boards used on the robot. The basic functionality of the boards and their role in the overall robot is described in more detail in Chapter 5. There are six pages for the analog force board, 2 pages for the signal conditioning board, 1 page for the analog breakout board, and 1 page for the power distribution board.



Title		MIT LEG LAB, BIPED FORCE BOARD	
Size	Document Number	Rev	(RevCode)
A	POWER AND CONNECTORS		
Date:	Tuesday, December 21, 1999	Sheet	1 of 6

Figure B-1: Page 1 of 6 of the biped force board.



Title		MIT LEG LAB, BIPEd FORCE BOARD	
Size	Document Number	Rev	(RevCode)
A	FORCE ERROR, A and B		
Date:	Wednesday, December 15, 1999	Sheet	2 of 6

Figure B-2: Page 2 of 6 the biped force board.

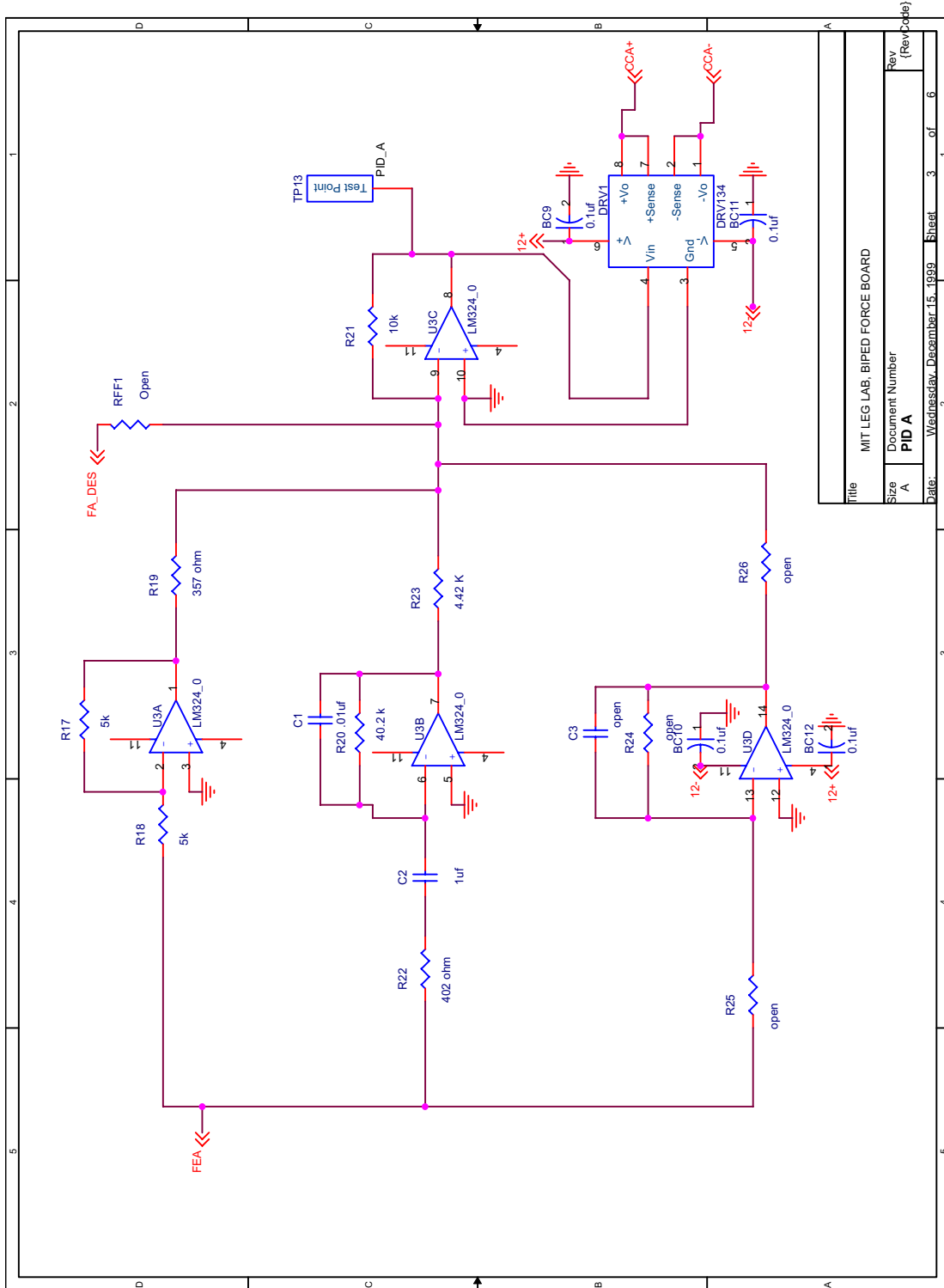
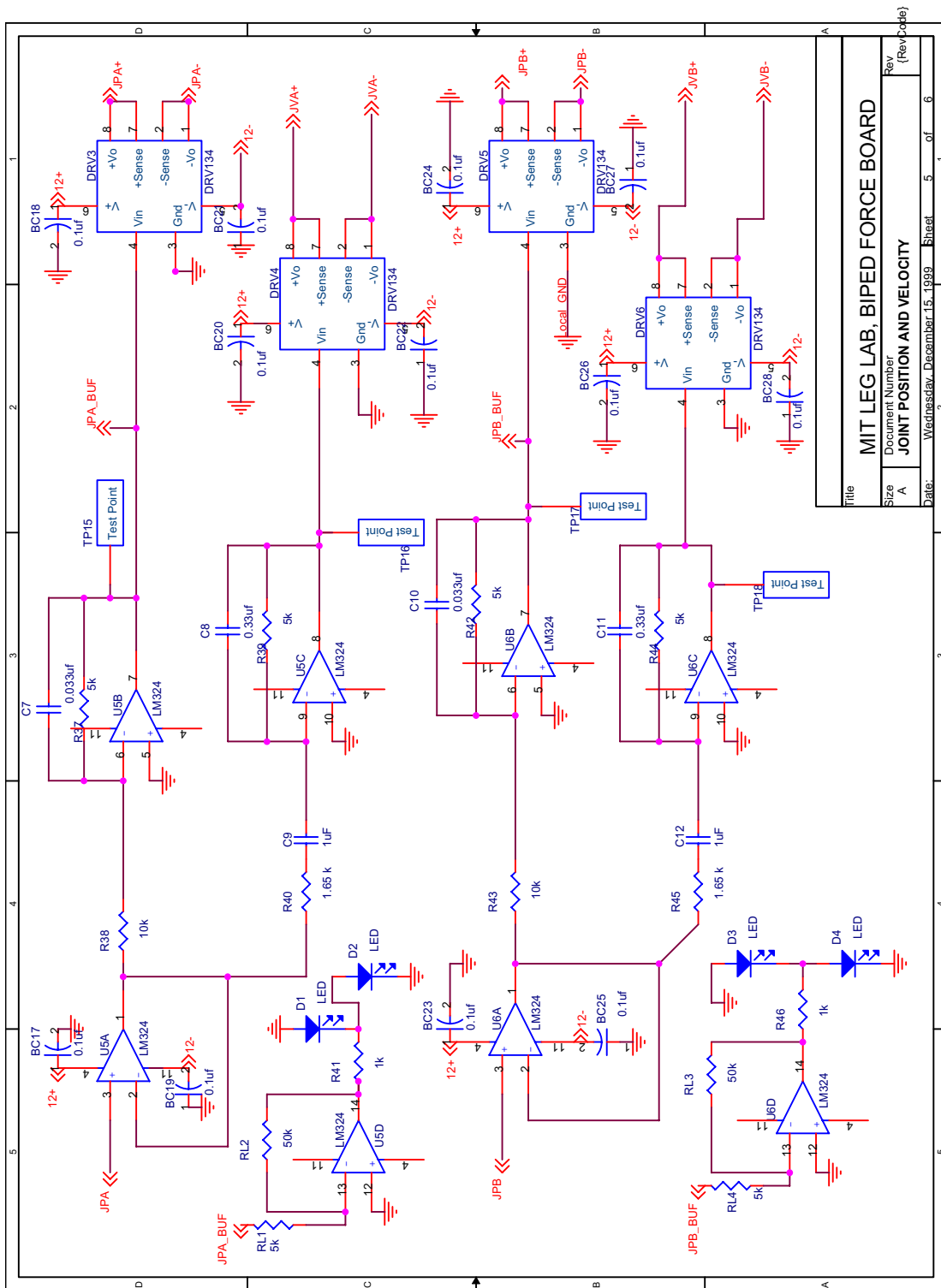


Figure B-3: Page 3 of 6 of the biped force board.



Title		MIT LEG LAB, BIPED FORCE BOARD	
Size	Document Number	Rev	(RevCode)
A	A	1	6
Date:	Wednesday, December 15, 1999	Sheet	5 of 6

Figure B-5: Page 5 of 6 of the biped force board.

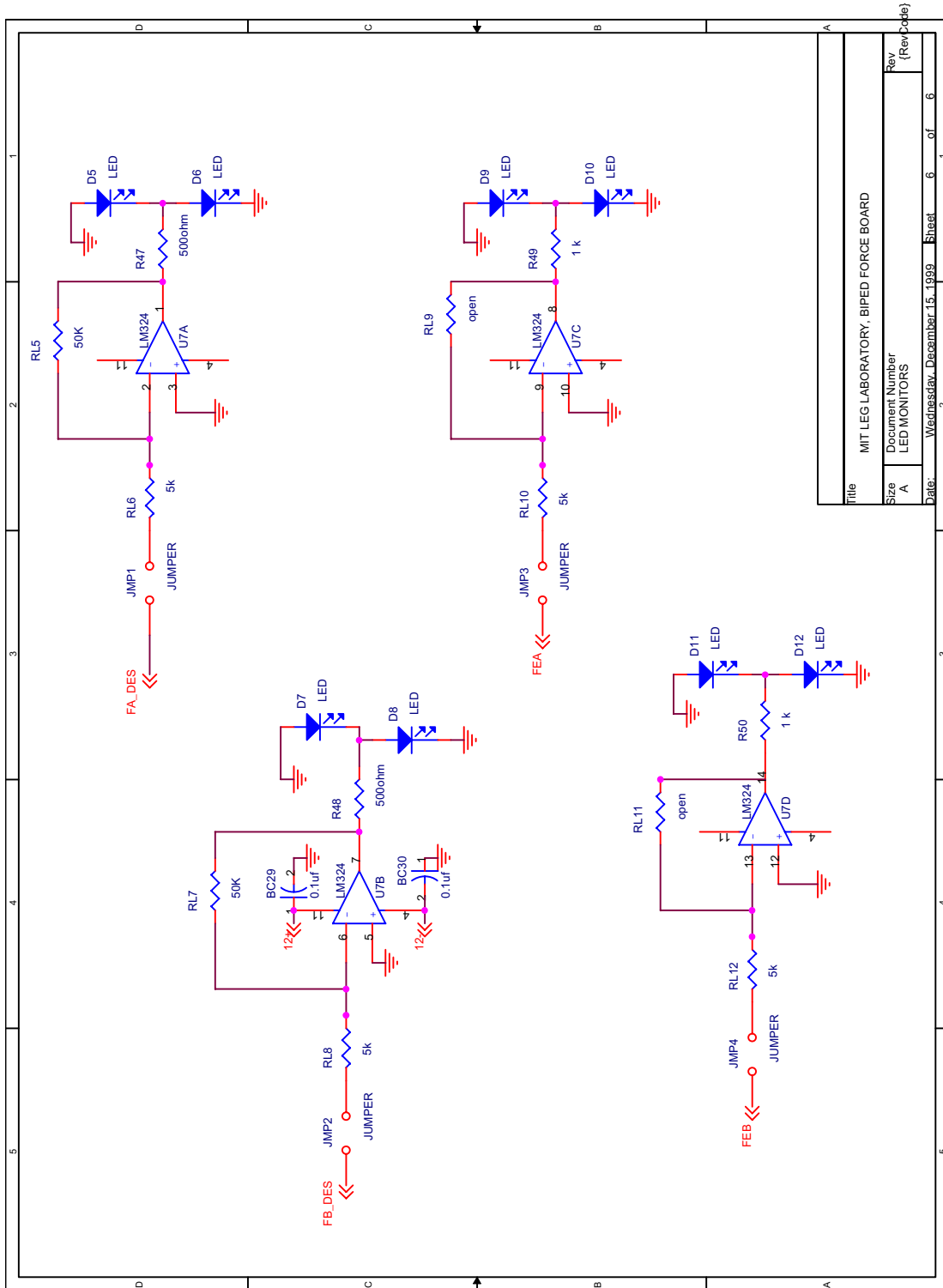


Figure B-6: Page 6 of 6 the biped force board.

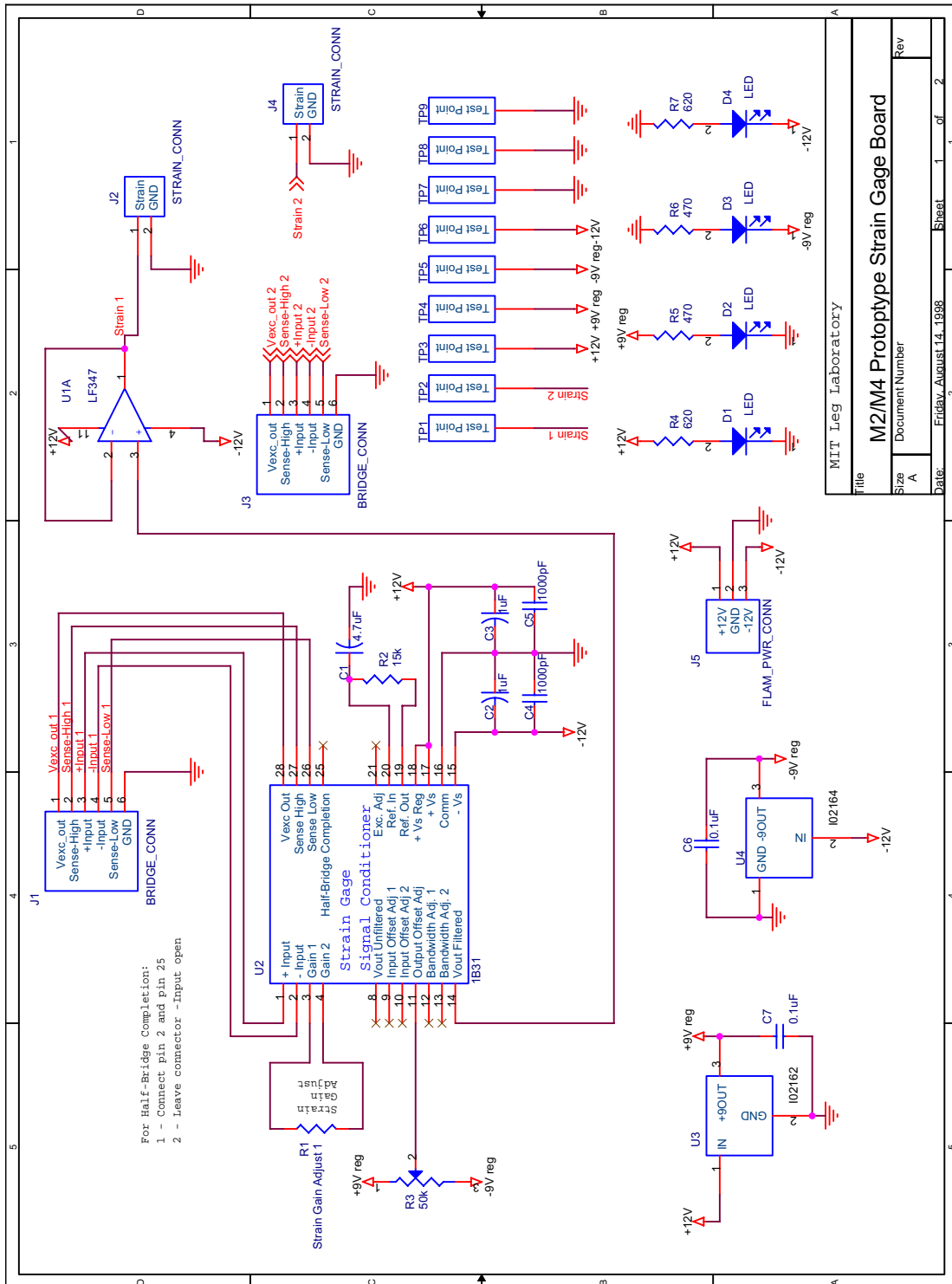
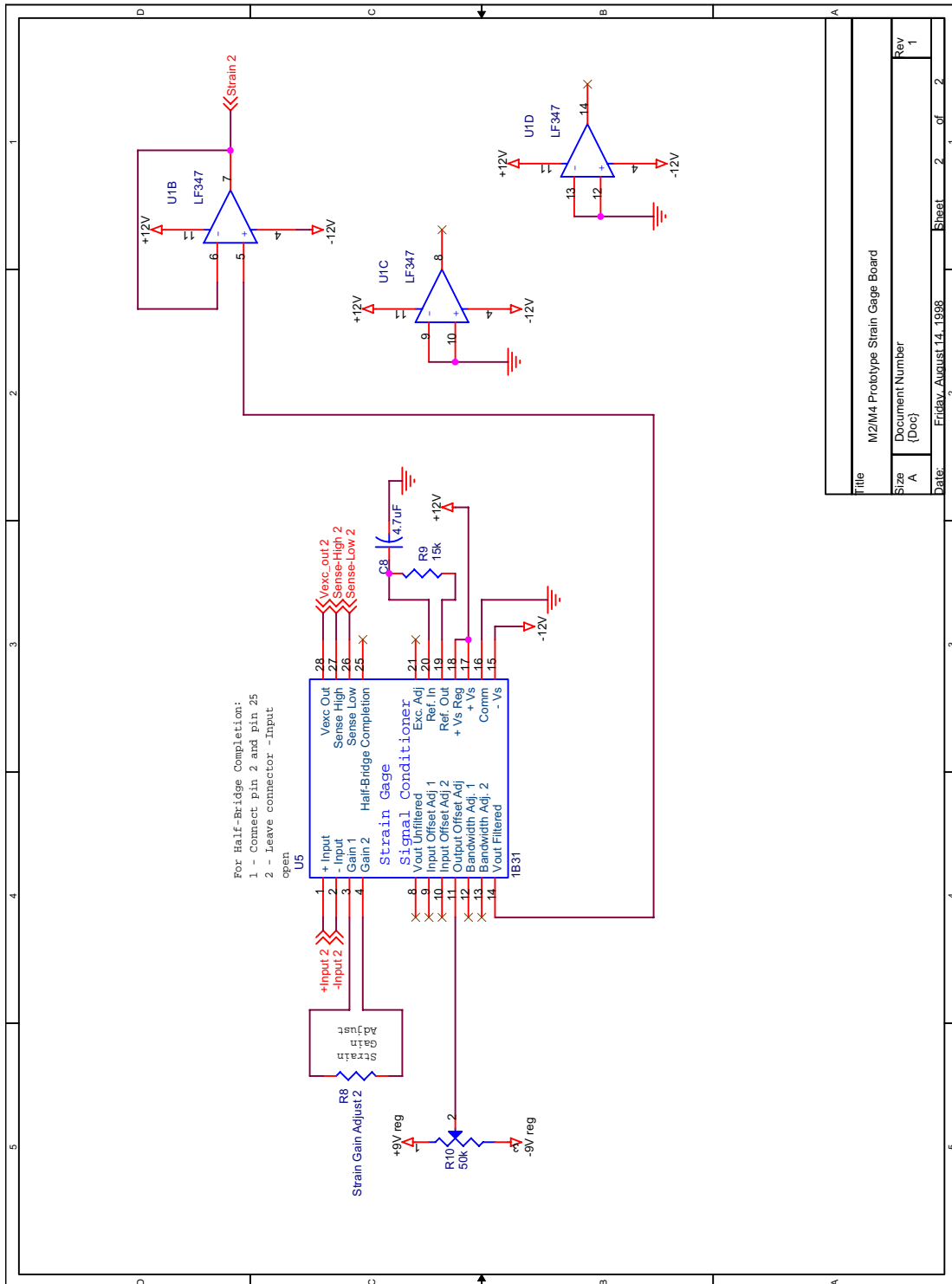


Figure B-7: Page 1 of 2 of the strain gauge conditioning board.



Title		M2M4 Prototype Strain Gauge Board	
Size	A	Document Number	Rev 1
Date:	Friday, August 14, 1998	Sheet	2 of 2

Figure B-8: Page 2 of 2 of the strain gauge conditioning board.

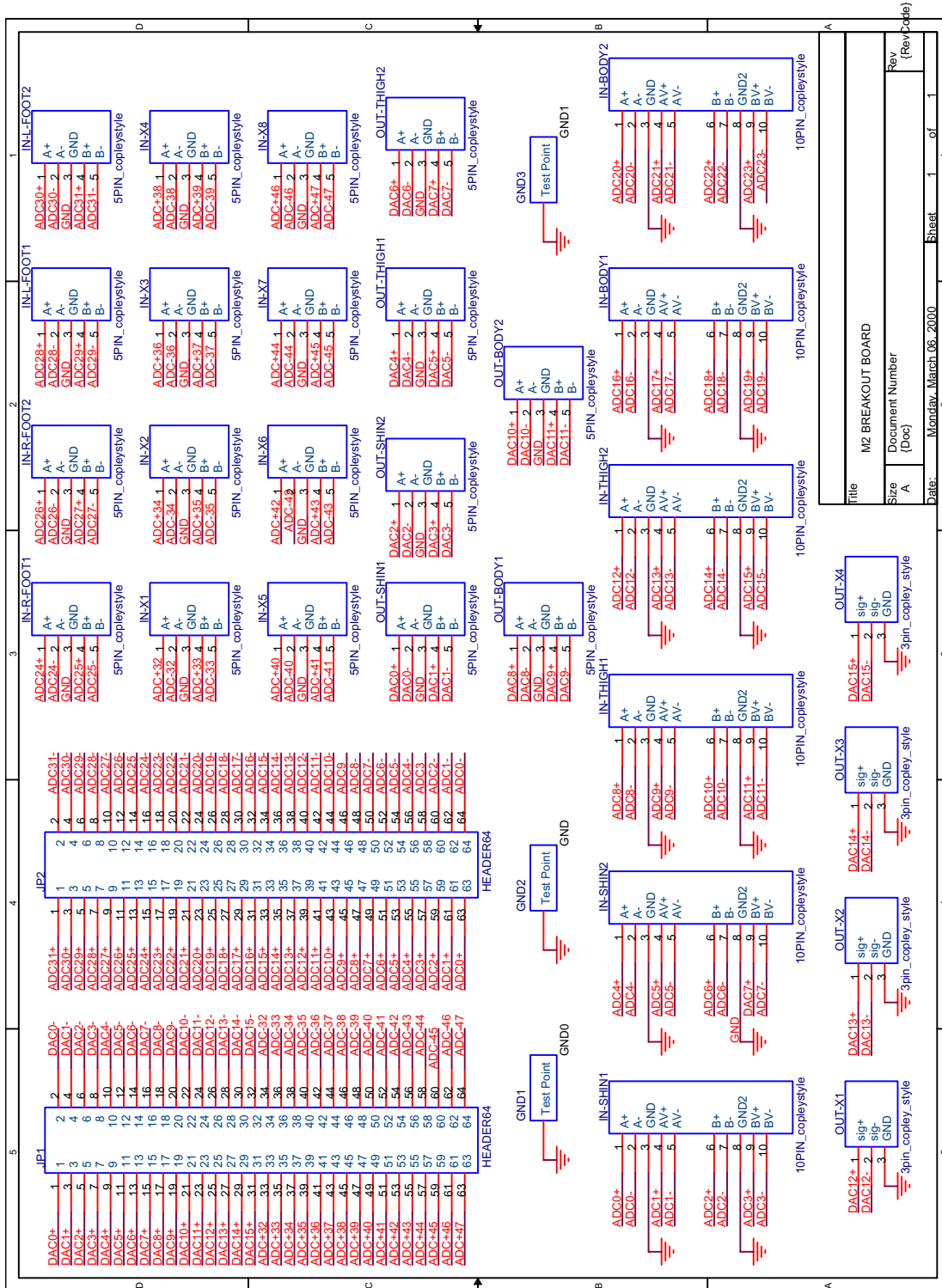


Figure B-9: Page 1 of 1 of the analog I/O breakout board. This board is designed to interface with the ANA070 and ANA064 from Digital Designs and Systems.

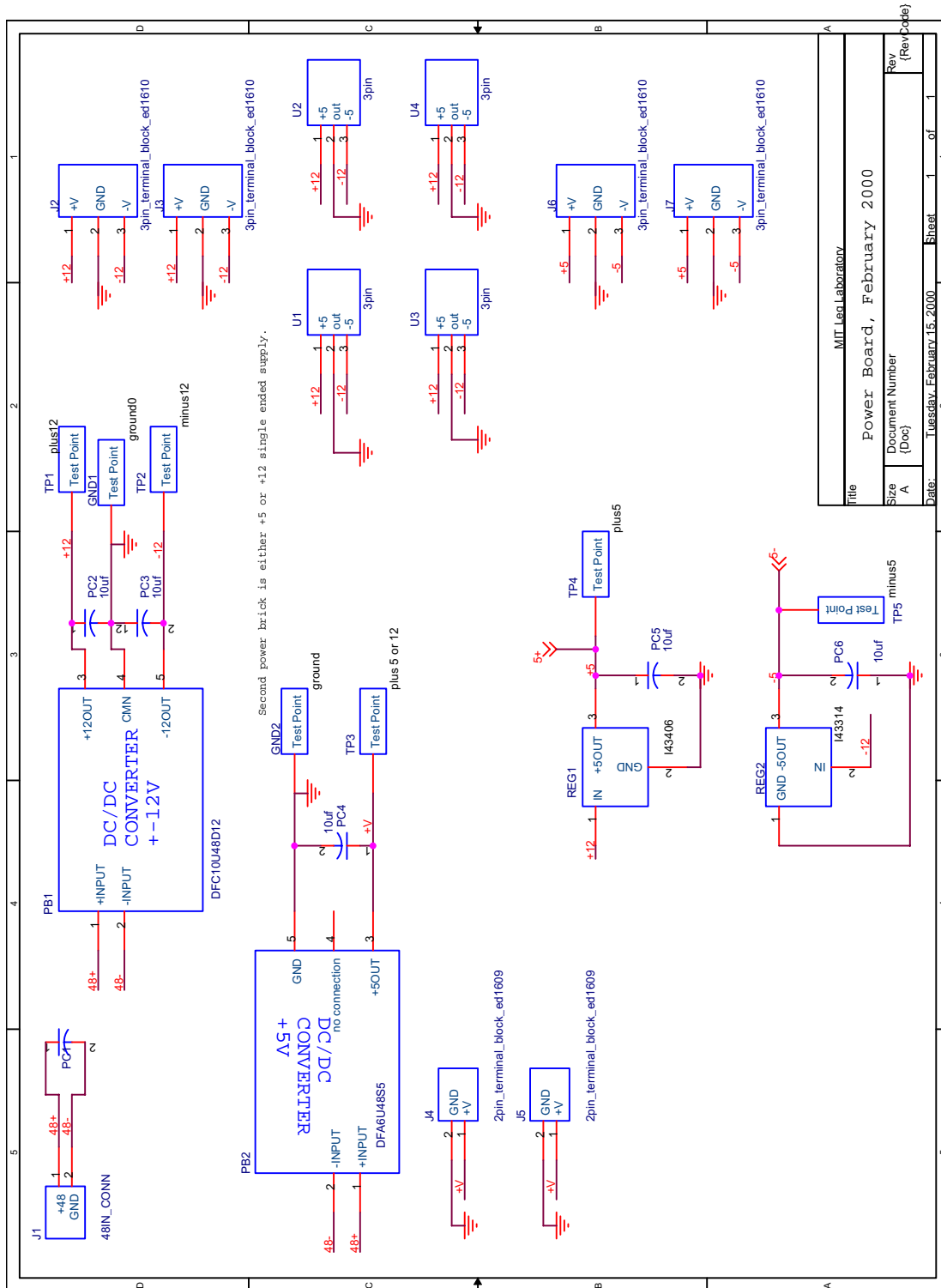


Figure B-10: Page 1 of 1 of the M2 power distribution board. This board has two different population options. One to power the DSP and one to power the Intersense IS-300 tracker.

Appendix C

Suppliers and Costs

This section contains a list of all the suppliers that were used in development of the robot.

Digital Designs and Systems
3266 North Meridian Street
Indianapolis, IN 46208
317-931-8190
<http://www.dideas.com/>
microcontrollers, a/d and d/a conversion, vision systems, ready built and custom designs

Stock Drive Products
2101 Jericho Turnpike,
Box 5416
New Hyde Park, NY 11042-5416
(516)328-3300
Mechanical Parts

Berg
499 Ocean Avenue
Box 130
East Rockaway, NY 11518
(516)596-1700
Mechanical Parts

NOVOTECHNIK
237 CEDAR HILL STREET
MARLBORO, MA 01752
(508) 485-2244
Potentiometers

SMALL PARTS INC
13980 NW 58TH COURT
PO BOX 4650
MIAMI LAKES, FL 33014-3115
(800) 220-4242
Mechanical Parts

CENTURY SPRING COMPANY INC
BOX 15287
222 EAST 16TH STREET

LOS ANGELES, CA 90015-0287
(800)237-5225
Springs

Newark Electronics
41 Pleasant Street
Methuen, MA 01844
(800) 463-9275
Electronic Parts

REC ENGINEERING COMPANY(Bob)
20 HOPKINS STREET
WILMINGTON, MA 01887-2210
(508)657-6517
Machining

Eastern Tool(Joe)
Somerville, MA
(617)497-6703
Machining

Transducer Techniques
43178 Business Pk. Dr.
Temecula CA 92590
1-800-344-3965
Load cells.

Intersense, Inc.
73 Second Avenue
Burlington MA 01803
(781)-270-0090
Multi-axis inclinometer.

Digi-Key Corporation
701 Brooks Ave. South
Thief River Falls, MN 56701-0677
(800)344-4539
Electronic Parts

Copley Controls Corporation
410 University Avenue
Westwood, MA 02090
(617)329-8200
FAX: (617)329-4055
Amplifiers

Cooner Wire Company
9265 Owensmouth
Chatsworth, CA 91311
(818)882-8311
Flexible Wire

CFC, Inc.
179 Bear Hill Road
Waltham, MA 02154-1001
(617)890-1878
FAX: (617)890-7098
MODEM: (617)890-7193
Circuit Board Fabrication

Advanced Circuits
Colorado, <http://www.4pcb.com>
Circuit Board Fabrication, online ordering

NSK -linear motion division
Elmhurst, IL 60126-1016
ATTN: Sandy x2638 or Jackie x2677
tel:1-800-255-4773
fax:630-924-8197
Ballscrews

Litton Poly-Scientific
1213 North Main Street
Blacksburg, VA 24060
(828)837-5115
Attn: Barbara Smith x231
fax (828)837-0846
Brushless DC motors

McMaster Carr
BOX 440
NEW BRUNSWICK, NJ 08903-0440
(908)329-3200
Mechanical Parts

QUALITY COMPOSITES INC
8385 S ALLEN STREET No.140
SANDY, UT 84070
(801)565-8003
FAX: (801)565-8225
Carbon Fiber Tubes

Sava Industries, Inc.
4 N. Corporate Drive, P.O. Box 30
Riverdale, NJ 07457-0030
(201) 835-0882
Steel Cable, crimps and crimp tools.

Tristar Plastics
Shrewsbury, MA
800.874.7827x3203(mike rudel)
fax 508.845.1200

Rulon bushings

W.S. Deans
10875 Portal Drive
Los Alamitos CA 90720
714-828-6494 Robin
Wet noodle wire

US Sensor Corp
1832 West Collins Ave.
Orange, CA 92867
714-639-1000
Terry ext 104
Thermal sensors for mounting amps to heat sinks

Tra-Con
45 Wiggins Ave.
Bedford, MA 01730
1.800.872.2261
781.275.6363
Glue for glueing thermal sensors to amp heat sink.

Tower Hobbies
PO Box 9078
Champaign, IL 61824-9078
1-800-637-6050
Batteries and charger

C.1 Costs

This section contains the costs associated with the robot M2. Costs and quantities given do not include spares. The general lab policy is to order 50 percent spares on everything. I think that anyone else developing a similar robot should do the same. See Table C.1 for details.

Component	QTY	Each US \$	Total US \$
Actuator, Amp	12	1500	18,000
Custom Computer	1	10,000	10,000
CFRP frame	8	300	2500
Machining	1	30,000	30,000
Vestibular	1	10,000	10,000
Misc Parts	200	20	4000
PCB's	10	1,000	10,000
Load Cells	8	450	3600
TOTALS			88,100

Table C.1: Basic robot budget. See Robinson et al.((17)) for more detail on the actuator. This budget does not include prototyping or development costs. Part quantities and individual costs are not necessarily meant to imply identical parts but rather to give an average price for all units of a certain type.